## This is to certify that the

### thesis entitled

An Analysis of the Settlement of Footings on Sand

presented by

Richard Wayne Christensen

has been accepted towards fulfillment of the requirements for

M.S. degree in Civil Engineering

Major professor

Date May 20, 1960

O·169



## AN ANALYSIS OF THE SETTLEMENT OF FOOTINGS ON SAND

Ву

### RICHARD WAYNE CHRISTENSEN

### AN ABSTRACT

Submitted to the College of Engineering of Michigan
State University of Agriculture and Applied
Science in partial fulfillment of the
requirements for the degree of

MASTER OF SCIENCE

Department of Civil Engineering

1960

Approved Muen

#### AN ABSTRACT

In this thesis, an attempt is made to formulate a rational method of analysis of the settlement of footings on sand.

Present methods of analysis are reviewed.

The problem undertaken is that of determining the stresses and settlement under a rigid continuous footing on sand. The method of settlement analysis developed is a numerical procedure based on the theory of elasticity.

It is assumed that the sand mass is elastic and isotropic but not homogeneous. A grid system is established for the sand mass and the displacement equations from theory of elasticity are written in finite difference form for each of the grid points. On the basis of triaxial tests, the modulus of elasticity of sand is taken as a function of the minor principal stress. The minor principal stress is evaluated and the values of E for each of the grid points are estimated. The displacement equations are then solved by the digital computer. The stresses at the grid points are then determined, also by the digital computer.

It was found that the contact pressure and settlement obtained in the numerical method agrees very well with the results of model tests.

## AN ANALYSIS OF THE SETTLEMENT OF FOOTINGS ON SAND

Ву

### RICHARD WAYNE CHRISTENSEN

# A THESIS

Submitted to the College of Engineering of Michigan
State University of Agriculture and Applied
Science in partial fulfillment of the
requirements for the degree of

MASTER OF SCIENCE

Department of Civil Engineering

# ACKNOWLEDGMENTS

The author wishes to express his most sincere thanks and appreciation to Dr. T. H. Wu, Department of Civil Engineering, Michigan State University whose expert guidance and encouragement helped make this study possible.

5-20-60

# TABLE OF CONTENTS

Section		Page	
ACKNOWLEDGMENTS			
LIST OF SYMBOLS			
I.	INTRODUCTION	1	
II.	ANALYTICAL METHODS OF PREDICTING SETTLEMENTS	5	
III.	DEVELOPMENT OF THE NUMERICAL METHOD	12	
IV.	SETTLEMENT ANALYSIS	20	
v.	CONCLUSIONS	24	
APPENDIX			
BIBLIOGRAPHY			

### LIST OF SYMBOLS

C = compression index

C = bearing capacity index

D = deviator stress

e = void ratio

E = modulus of elasticity

G = modulus of elasticity in shear

h = depth of significant stress

p = pressure intensity

U = horizontal displacement

V = vertical displacement

€ = unit strain

γ = unit weight of soil

 $\rho$  = settlement

σ = normal stress

 $\sigma_1$  = major principal stress

 $\sigma_3$  = minor principal stress

 $\mu$  = Poisson's ratio

φ = effective angle of internal friction

 $\phi_{:}$  = angle of obliquity

#### I. INTRODUCTION

## Stresses and Displacements

In 1885, the French mathematician Boussinesq (2) applied the theory of elasticity to the problem of a concentrated load acting on a semi-infinite solid. He obtained the following solution for the stresses (Figure 1).

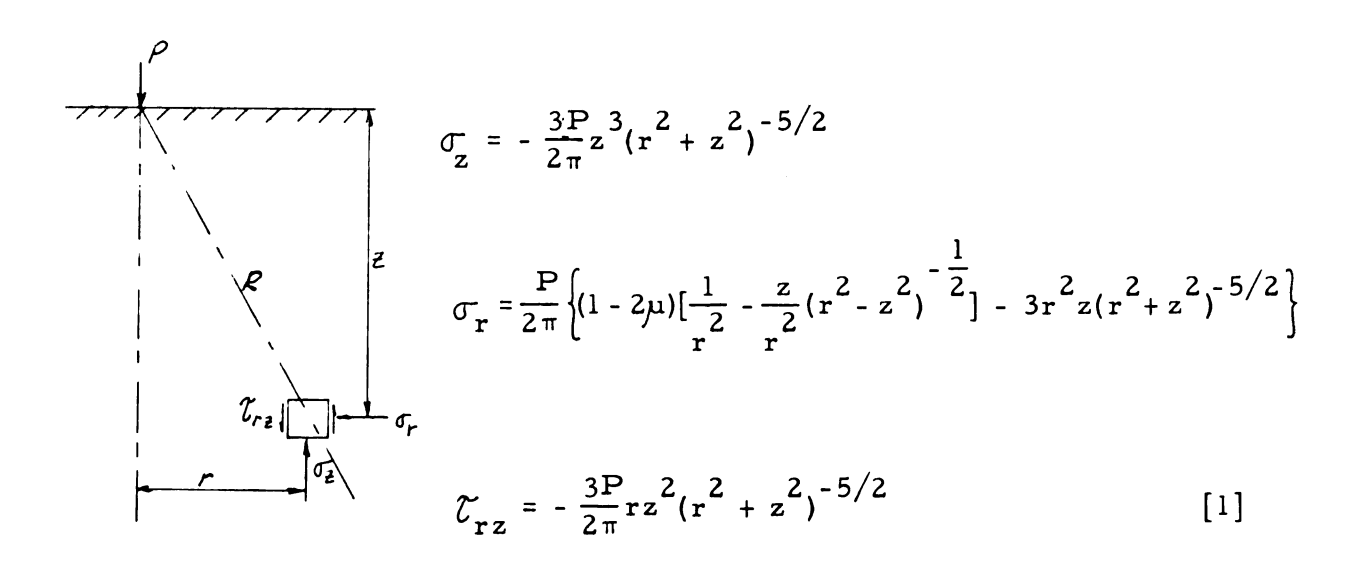


Figure 1: Diagram illustrating the symbols of the Boussinesq equations.

These equations are known as Boussinesq's equations. They indicate, in a general way, the stress distribution that might be expected in a soil mass when its depth is large compared to the dimensions of the loaded area. Experimental evidence indicates that this stress distribution is approximately correct for most soils. [See for instance Jurgenson (5).]

		 er v <del>allered</del>

If the theory of elasticity approach is extended to the case of a circular, uniformly loaded area of radius r, it is found that the vertical stress beneath the center of the loaded area is given by

$$\sigma_{\mathbf{z}} = p \left[ -1 + \frac{\mathbf{z}^3}{(\mathbf{r}^2 + \mathbf{z}^2)^{3/2}} \right]$$
 [2]

where p is the intensity of the load.

The settlements produced by the flexible, uniform load on the surface of a semi-infinite elastic solid have also been computed by elasticity methods. For a square loaded area, if  $\mu$  is assumed to be 0.5, the settlement is (9)

$$\rho_{\text{cor}} = \frac{.42 \text{pb}}{E}$$

$$\rho_{\text{cen}} = \frac{.84 \text{pb}}{E}$$
[3]

where  $\rho$ cor = settlement at the corner of the loaded area

Pcen = settlement at the center of the loaded area

p = intensity of load

b = width of loaded area

E = modulus of elasticity of the solid

The general shape of the settlement profile resulting from the application of a uniform load is shown in Figure 2. This is the case if the load is perfectly flexible.

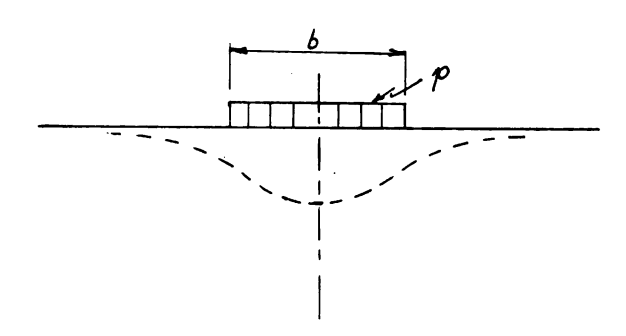


Figure 2: Settlement profile for a flexible, uniform load on a semi-infinite elastic solid.

If a load is applied to a semi-infinite elastic solid by a perfectly rigid footing, the pressure on the base of the footing will not be uniform. The solution of the problem by the theory of elasticity results in the pressure distribution shown below.

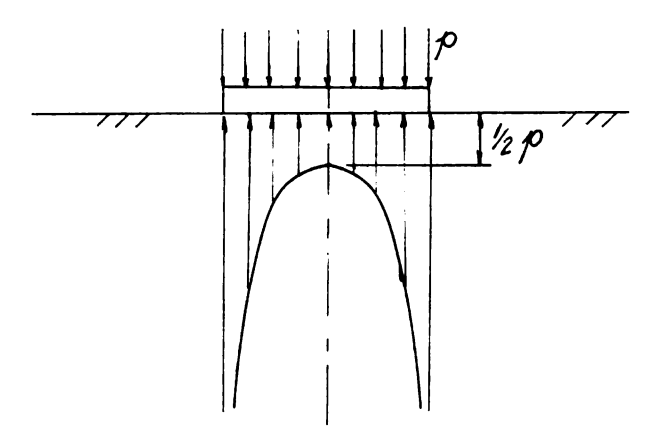


Figure 3: Pressure distribution on a rigid footing on a semi-infinite elastic solid.

The settlement of the rigid footing is found to be about 7.3 per cent smaller than the average settlement of a flexible footing of the same area, acted on by an equal intensity of load p.

# Limitations of Elastic Theory

The preceding discussion treats the stresses and displacements in a semi-infinite elastic solid under the application of various types of loading. This of course assumes that the material subjected to stress is elastic, homogeneous, and isotropic. It is well known that such is not the case with soils, particularly sand. If a sample of elastic material has acting on it the principal stresses  $\sigma_1$ ,  $\sigma_2$ , and  $\sigma_3$  and one of the principal stresses is increased, the resulting strain is independent of the initial principal stresses. However, for sand, the strain is dependent to a very large extent on the initial principal stresses. It decreases as the initial principal stresses are increased. In a mass of sand, the confining pressure increases with depth due to the weight of the overburden. It may therefore be concluded that a mass of sand is elastically nonhomogeneous in the vertical direction.

At great depths in a sand mass, where the confining pressure is large, the variation in the ratio of applied stress to strain is small. However, near the surface of a sand stratum, the assumption of proportionality between stress and strain which does not change with depth is far from correct.

It should also be noted that Poisson's ratio is not constant for granular soils. It may increase from 0.2 at low stresses to more than 0.5 at high stresses.

In light of these facts, it becomes obvious that the elasticity

solutions which are based on the assumption of isotropy and homogeneity of the material are not applicable to the problem of the settlement of footings on sand.

Because of the large number of variables and the mathematical difficulties involved, the approach to the problem of settlement of footings on sand in the past has been primarily empirical. This approach has usually consisted of the accumulation of data relating the observed settlement of footings to some readily measurable soil property such as the relative density (or resistance to the penetration test). (10) The results of these data are presented in the form of design charts. The charts are very conservative and their use generally results in a safe design. However, in exceptional cases (such as a very loose sand) they may give results on the unsafe side. It is therefore desirable to develop a more fundamental understanding of the mechanism of settlement.

# II. ANALYTICAL METHODS OF PREDICTING SETTLEMENT

# Elastic Analysis

It is assumed that the stress distribution below a uniformly loaded, flexible footing is close to that computed from the theory of elasticity. The elastic constants necessary for settlement calculations can be determined from the triaxial test.

The vertical unit strain in an elastic material is given by

$$\epsilon_{y} = \frac{\Delta \sigma}{E} - \frac{\mu}{E} (\Delta \sigma_{2} + \Delta \sigma_{3})$$
 [4a]

where E = modulus of elasticity and  $\mu$  = Poisson's ratio. In the triaxial test,  $\sigma_2$  =  $\sigma_3$  so

$$\epsilon_{y} = \frac{\Delta \sigma_{1}}{E} - 2\mu \frac{\Delta \sigma_{3}}{E}$$
 [4b]

This expression may be written in slightly different form as follows.

$$\epsilon_{y} = \frac{\Delta \sigma}{E} - 2\mu \frac{\Delta \sigma}{E} + \frac{\Delta \sigma}{E} - \frac{\Delta \sigma}{E}$$
 or

$$\epsilon_{v} = (\frac{1}{E} - \frac{2\mu}{E}) \Delta \sigma_{3} + \frac{1}{E} (\Delta \sigma_{1} - \Delta \sigma_{3})$$
 [4c]

Equation [4c] can be expressed as

$$\epsilon_{y} = \frac{\Delta h}{h} = C_{III} \cdot \Delta \sigma_{3} + C_{I}(\Delta \sigma_{1} - \Delta \sigma_{3})$$
 [5]

where

$$C_{I} = \frac{1}{E}$$
 and  $C_{III} = (\frac{1}{E} - \frac{2\mu}{E})$ 

h = thickness of layer considered

 $\Delta h$  = change in thickness i. e. settlement of layer considered

The elastic constants  $C_I$  and  $C_{III}$  can be determined by two sets of triaxial tests. To determine  $C_I$ , the lateral pressure is held constant  $(\Delta\sigma_3=0)$  and the deviator stress  $(\Delta\sigma_1-\Delta\sigma_3)$  is increased. Then

 $C_{I} = \frac{\epsilon_{y}}{(\Delta\sigma_{1}^{2} - \Delta\sigma_{3}^{2})}$  which is the slope of the deviator stress versus axial strain curve. To evaluate  $C_{III}$ , the deviator stress is held constant  $(\Delta\sigma_{1}^{2} - \Delta\sigma_{3}^{2} = 0)$ . Then  $C_{III} = \frac{1}{E}$ , which is the slope of the lateral pressure  $(\sigma_{3}^{2})$  versus axial strain curve.

As was pointed out earlier,  $\mu$  and E for sand are not constants, but vary with the confining pressure. In order to account for this fact, the laboratory specimens should be tested under initial values of  $\sigma_1$  and  $\sigma_3$  appropriate for the depth of the points under consideration. The values of  $C_I$  and  $C_{III}$  are then representative of that attainable in the sand at the various depths.

$$\rho = \Sigma \left\{ C_{III} \cdot \Delta \sigma_3 + C_I (\Delta \sigma_1 - \Delta \sigma_3) \right\} h$$
 [6]

where  $\rho$  = settlement of the footing and h = height of each individual layer.

The changes in the principal stresses  $\Delta\sigma_3$  and  $\Delta\sigma_1$  caused by the load are determined from Boussinesg's equations.

## Plastic Analysis

In a thesis presented in 1956, Bond (1) developed a method, based on plastic theory, of predicting the settlement of circular footings on sand.

The state of stress on a vertical line beneath the center of a circular foundation is expressed as

$$\sigma_{1} = \sigma_{3} \tan^{2}(\frac{\pi}{4} + \frac{\Phi_{e}}{2})$$
 [7]

when  $\phi_{e}$  = partially mobilized angle of internal friction.

The value of  $\varphi_{\mathbf{e}}$  at any point beneath the center of the footing is calculated assuming that potential surfaces of failure develop as shown below.

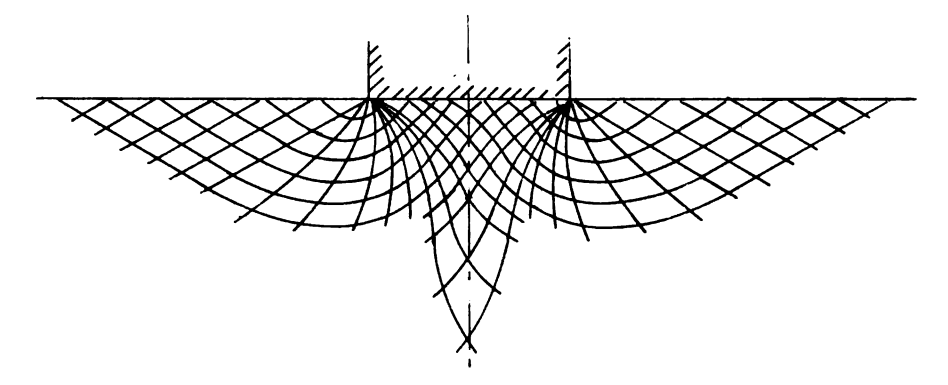


Figure 4: Probable shear pattern beneath a rigid, circular footing on a dry sand. [After Bond (1).]

The value of  $\phi_e$  is assumed constant along any particular failure surface. The vertical stress along the centerline is calculated by Boussinesq's equation. Triaxial tests were used to determine the stress-strain characteristics of a typical sand. The test results

were expressed in a plot of  $\phi_e$  versus vertical strain for various values of  $\sigma_l$  where  $\phi_e$  is determined by equation [7].

Having the values of  $\sigma$  and  $\phi$  at a particular point, the stress-strain curves can be used to find the vertical strain  $\varepsilon$  at the point. Integration of the strain along the centerline gives the settlement of the footing at that point.

Comparison of Bond's theoretical calculation of  $\phi_e$  beneath the center of the footing with experimental results obtained by the Waterways Experiment Station (13) shows good agreement. However, the experimental results are not in good agreement with the values of  $\phi_e$  as determined by Boussinesg's equation and equation [7].

Experimental results obtained by Bond show good agreement between measured vertical stress and the vertical stress as calculated by Boussinesq's equation. The settlements determined from these tests agree with theoretical calculations for dense sand but not for loose sand. It is obvious that the failure pattern assumed in the plastic analysis does not develop in the case of loose sand. [See Myerhoff (6).]

## Consolidation

Hough (4) has presented a method, based on volume changes in one-dimensional compression, for predicting settlements of footings on any type of soil.

In a one-dimensional consolidation test, a relationship between the void ratio and the applied pressure is obtained. It is usually plotted on a semi-log graph. (See Figure 5.)

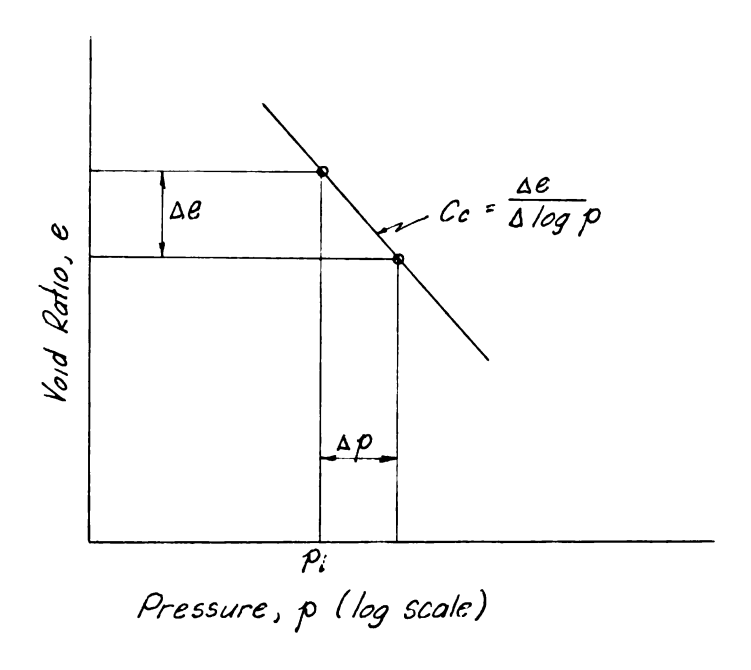


Figure 5: Compression diagram. [After Hough (4).]

The slope of the pressure-void ratio curve is called the compression index ( $C_c$ ). The change in void ratio  $\Delta e$  for any increment of pressure increase  $\Delta p$  is given by the equation

$$\Delta e = C_c \log (1 + \frac{\Delta p}{P_i})$$
 [8]

where  $p_i$  = initial vertical pressure on the element. The change in thickness  $\Delta h$  of a soil layer with an initial thickness of h is

$$\Delta h = h \frac{\Delta e}{1 + e_0}$$
 [9]

where  $e_0$  = initial void ratio. Equations [8] and [9] may be combined to obtain the following expression for the change in thickness of a soil layer

$$\Delta h = h \frac{C_c}{1 + e_o} \log \left(1 + \frac{\Delta p}{p_i}\right)$$
 [10]

For the purpose of simplifying the notation, the following substitutions are introduced.

Let 
$$\frac{1 + e_0}{C_c} = C = \text{bearing capacity index}$$

and 
$$\Delta h = \rho = settlement$$

Equation [10] may then be expressed as

$$\Delta p = (10^{\frac{C}{h}} - 1) p_i$$
 [11]

By combining the foregoing basic relationships from the consolidation test, Hough obtained an equation relating the settlement of a footing to the contact pressure.

$$p_{c} = \frac{\gamma}{27B^{2}} h_{s} (10^{\frac{h_{s}}{h_{s}}} - 1) (h_{s} + 3B)^{2}$$
 [12]

where  $h_s$  is defined as the depth of significant stress and is determined by

$$h_s (h_s + B)^2 = \frac{10B^2}{Y} p_c$$
 [12a]

and B = width of footing,  $p_C$  = average contact pressure. These expressions are based on the assumed pressure distribution shown in Figure 6.

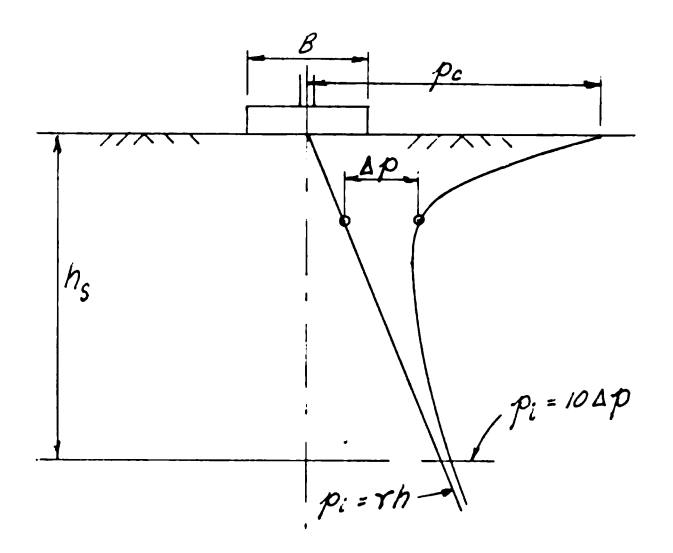


Figure 6: Variation of stress with depth. [After Hough (4).]

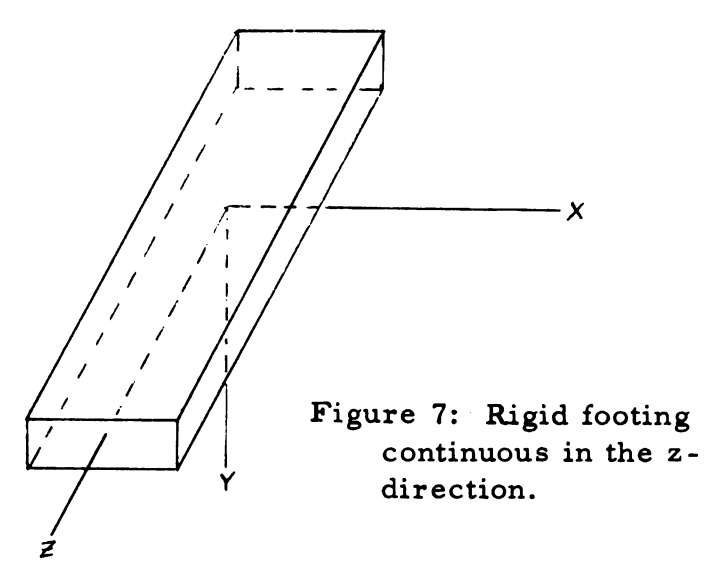
Observation of the conditions imposed on the sample in the consolidation test reveals serious shortcomings in this method of settlement analysis when applied to sands. In the consolidation test, the sample is compressed under the condition of zero lateral strain, while in the case of sand beneath a loaded footing, considerable lateral strain may develop. Therefore this method completely eliminates that part of the settlement contributed by lateral displacements.

Settlements calculated by this method are apt to be too low, particularly in the case of loose sand where the effect of lateral strain is significant.

# III. DEVELOPMENT OF THE NUMERICAL METHOD

## Displacement Equations

One considers the case of a continuous, rigid footing acting on a semi-infinite mass of sand. It is assumed for the present that the sand is elastic, but not homogeneous.



Since the footing is continuous in the z-direction the problem can be treated as one of plane strain ( $\xi_z = 0$ ). Then from elastic theory, Hooke's Law is

$$\sigma_{\mathbf{x}} = \lambda \mathbf{e} + 2\mathbf{G} \in_{\mathbf{x}} \qquad \text{where} \qquad \lambda = \frac{\mu \mathbf{E}}{(1+\mu)(1-2\mu)}$$

$$\sigma_{\mathbf{y}} = \lambda \mathbf{e} + 2\mathbf{G} \in_{\mathbf{y}} \qquad [13] \qquad \mathbf{e} = \in_{\mathbf{x}} + \in_{\mathbf{y}}$$

$$\tau_{\mathbf{x}\mathbf{y}} = \tau_{\mathbf{y}\mathbf{x}} = \mathbf{G} \gamma_{\mathbf{x}\mathbf{y}} \qquad \mathbf{G} = \frac{\mathbf{E}}{2(1+\mu)}$$

In the two-dimensional problem  $\epsilon_{\mathbf{x}} = \frac{\partial \mathbf{U}}{\partial \mathbf{x}}$  and  $\epsilon_{\mathbf{y}} = \frac{\partial \mathbf{V}}{\partial \mathbf{y}}$  and  $\gamma_{\mathbf{x}\mathbf{y}} = (\frac{\partial \mathbf{U}}{\partial \mathbf{y}} + \frac{\partial \mathbf{V}}{\partial \mathbf{x}})$ , so that the Hooke's Law equations may be written in the following form.

$$\sigma_{\mathbf{x}} = \lambda e + 2G \frac{\partial U}{\partial \mathbf{x}} \qquad \qquad \sigma_{\mathbf{x}y} = \sigma_{\mathbf{y}x} = G(\frac{\partial U}{\partial \mathbf{y}} + \frac{\partial V}{\partial \mathbf{x}})$$

$$\sigma_{\mathbf{y}} = \lambda e + 2G \frac{\partial V}{\partial \mathbf{y}} \qquad [13a]$$

in which U and V are the displacements in the x and y directions respectively.

The equations of equilibrium for the two-dimensional problem in elasticity are

$$\frac{\partial \sigma_{\mathbf{x}}}{\partial \mathbf{x}} + \frac{\partial \mathcal{I}_{\mathbf{x}\mathbf{y}}}{\partial \mathbf{y}} + \mathbf{X} = 0 \qquad \text{where } \mathbf{X} = \text{body force in } \mathbf{x}\text{-direction}$$

$$\frac{\partial \sigma_{\mathbf{y}}}{\partial \mathbf{y}} + \frac{\partial \mathcal{I}_{\mathbf{x}\mathbf{y}}}{\partial \mathbf{x}} + \mathbf{Y} = 0 \qquad \qquad \mathbf{Y} = \text{body force in } \mathbf{y}\text{-direction}$$

By taking the partial derivatives of the Hooke's Law equations, the following expressions are obtained.

$$\frac{\partial \sigma_{\mathbf{x}}}{\partial \mathbf{x}} = \frac{\partial (\partial \mathbf{e})}{\partial \mathbf{x}} + 2 \frac{\partial}{\partial \mathbf{x}} (\mathbf{G} \frac{\partial \mathbf{U}}{\partial \mathbf{x}})$$

$$\frac{\partial \sigma_{\mathbf{y}}}{\partial \mathbf{y}} = \frac{\partial (\partial \mathbf{e})}{\partial \mathbf{y}} + 2 \frac{\partial}{\partial \mathbf{y}} (\mathbf{G} \frac{\partial \mathbf{V}}{\partial \mathbf{y}})$$

$$\frac{\partial \mathcal{E}_{\mathbf{x}\mathbf{y}}}{\partial \mathbf{x}} = \frac{\partial}{\partial \mathbf{x}} [\mathbf{G} (\frac{\partial \mathbf{U}}{\partial \mathbf{y}} + \frac{\partial \mathbf{V}}{\partial \mathbf{x}})]$$

$$\frac{\partial \mathcal{E}_{\mathbf{x}\mathbf{y}}}{\partial \mathbf{y}} = \frac{\partial}{\partial \mathbf{y}} [\mathbf{G} (\frac{\partial \mathbf{U}}{\partial \mathbf{y}} + \frac{\partial \mathbf{V}}{\partial \mathbf{x}})]$$
[15]

The body forces X and Y are assumed to be zero. Substituting equations [15] into [14] one obtains the displacement equations for the problem.

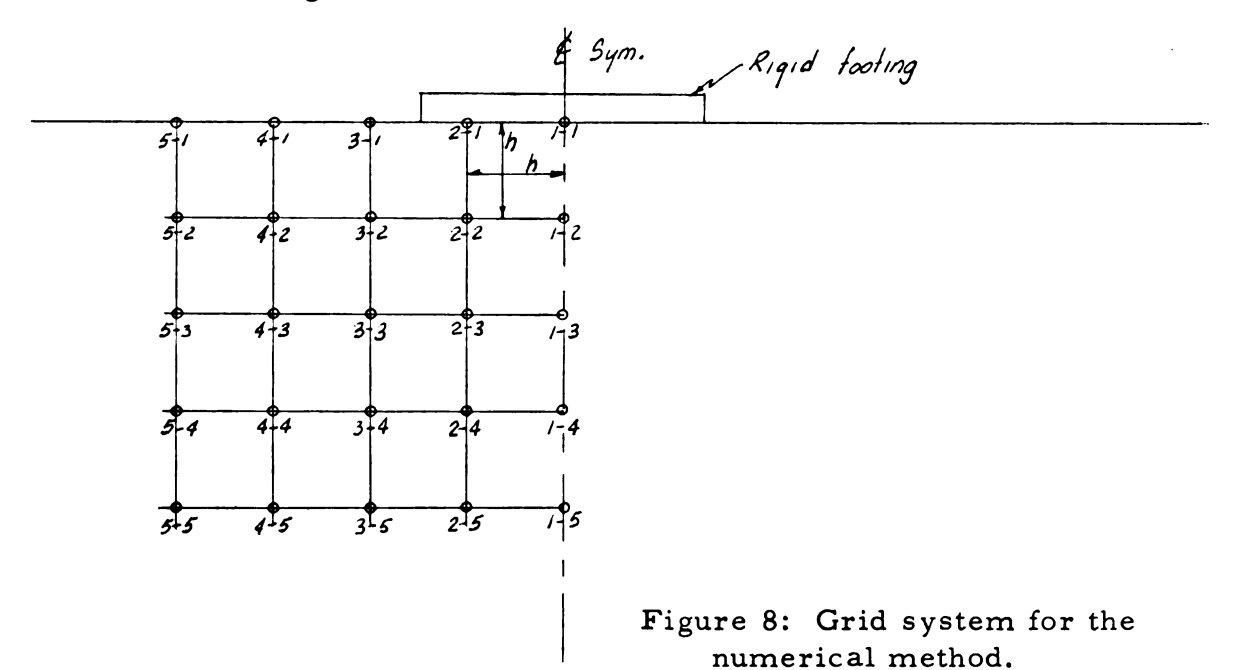
$$\frac{\partial}{\partial \mathbf{x}} \left[ \partial \left( \frac{\partial \mathbf{U}}{\partial \mathbf{x}} + \frac{\partial \mathbf{V}}{\partial \mathbf{y}} \right) \right] + 2 \frac{\partial}{\partial \mathbf{x}} \left( \mathbf{G} \frac{\partial \mathbf{U}}{\partial \mathbf{x}} \right) + \frac{\partial}{\partial \mathbf{y}} \left[ \mathbf{G} \left( \frac{\partial \mathbf{U}}{\partial \mathbf{y}} + \frac{\partial \mathbf{V}}{\partial \mathbf{x}} \right) \right] = 0$$
or 
$$\frac{\partial}{\partial \mathbf{x}} \left[ (\partial + 2\mathbf{G}) \frac{\partial \mathbf{U}}{\partial \mathbf{x}} + \partial \frac{\partial \mathbf{V}}{\partial \mathbf{y}} \right] + \frac{\partial}{\partial \mathbf{y}} \left[ \mathbf{G} \left( \frac{\partial \mathbf{U}}{\partial \mathbf{y}} + \frac{\partial \mathbf{V}}{\partial \mathbf{x}} \right) \right] = 0$$
[16a]

and 
$$\frac{\partial}{\partial y} \left[ \lambda \left( \frac{\partial U}{\partial x} + \frac{\partial V}{\partial y} \right) \right] + 2 \frac{\partial}{\partial y} \left( G \frac{\partial V}{\partial y} \right) + \frac{\partial}{\partial x} \left[ G \left( \frac{\partial U}{\partial y} + \frac{\partial V}{\partial x} \right) \right] = 0$$

or 
$$\frac{\partial}{\partial y} [(\gamma + 2G) \frac{\partial V}{\partial y} + \gamma \frac{\partial U}{\partial x}] + \frac{\partial}{\partial x} [G(\frac{\partial U}{\partial y} + \frac{\partial V}{\partial x})] = 0$$
 [16b]

Equations [16a] and [16b] may be written in terms of finite differences.

A grid system as shown in Figure 8 is set up for the soil mass beneath the loaded footing.



For any point o in the grid (Figure 9), the central difference expressions are as follows.

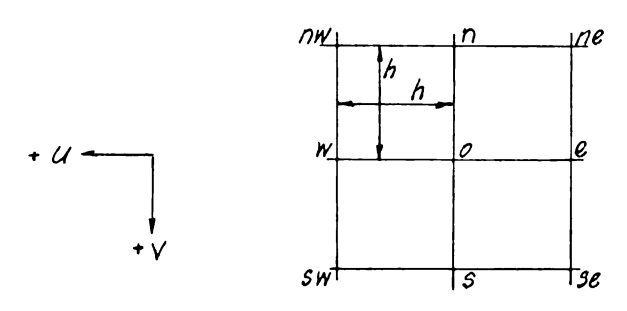


Figure 9: Finite difference notation.

$$\frac{\partial}{\partial \mathbf{x}} \left[ (\lambda + 2G) \frac{\partial \mathbf{U}}{\partial \mathbf{x}} \right] = \frac{a_{\mathrm{w,o}} \left( \frac{\mathbf{U}_{\mathrm{w}} - \mathbf{U}_{\mathrm{o}}}{\mathbf{h}} \right) - a_{\mathrm{e,o}} \left( \frac{\mathbf{U}_{\mathrm{o}} - \mathbf{U}_{\mathrm{e}}}{\mathbf{h}} \right)}{\mathbf{h}} = \frac{1}{\mathbf{h}^{2}} \left[ a_{\mathrm{w,o}} \left( \mathbf{U}_{\mathrm{w}} - \mathbf{U}_{\mathrm{o}} \right) - a_{\mathrm{e,o}} \left( \mathbf{U}_{\mathrm{o}} - \mathbf{U}_{\mathrm{e}} \right) \right]$$

$$\frac{\partial}{\partial x} (\lambda \frac{\partial V}{\partial y}) = \frac{\lambda_{w} (\frac{V_{sw} - V_{nw}}{2h}) - \lambda_{e} (\frac{V_{se} - V_{ne}}{2h})}{2h} = \frac{1}{4h^{2}} [\lambda_{w} (V_{sw} - V_{nw}) - \lambda_{e} (V_{se} - V_{ne})]$$

Similarly,

$$\frac{\partial}{\partial y}(G\frac{\partial U}{\partial y}) = \frac{1}{h^2}[G_{o, s}(U_s - U_o) - G_{n, o}(U_o - U_n)]$$

$$\vdots$$

$$\frac{\partial}{\partial x}(G\frac{\partial V}{\partial x}) = \frac{1}{h^2}[G_{o, w}(V_w - V_o) - G_{e, o}(V_o - V_e)]$$

where  $a = \lambda + 2G$ 

Substitution of the finite difference expressions into equations [16a] and [16b] gives

$$-2(a_0 - G_0)U_0 + \frac{1}{2}(a_w + a_0)U_w + \frac{1}{2}(G_0 - G_0)U_s + \frac{1}{2}(a_0 + a_0)U_e + \frac{1}{2}(G_0 + G_0)U_n$$

$$+\frac{1}{4}(\lambda_{w} + G_{s})V_{sw} - \frac{1}{4}(\lambda_{e} + G_{s})V_{se} + \frac{1}{4}(\lambda_{e} + G_{n})V_{ne} - \frac{1}{4}(\lambda_{w} + G_{n})V_{nw} = 0$$
 [17a]

$$-2(a_{o} + G_{o})V_{o} + \frac{1}{2}(G_{o} + G_{w})V_{w} + \frac{1}{2}(a_{o} + a_{s})V_{s} + \frac{1}{2}(G_{e} + G_{o})V_{e} + \frac{1}{2}(a_{n} + a_{o})V_{n}$$

$$+\frac{1}{4}(\lambda_{s} + G_{w})U_{sw} - \frac{1}{4}(\lambda_{s} + G_{e})U_{se} + \frac{1}{4}(\lambda_{n} + G_{e})U_{ne} - \frac{1}{4}(\lambda_{n} + G_{w})U_{nw} = 0$$
 [17b]

These two expressions are the displacement equations from theory of elasticity expressed in finite difference form. They apply in general to any point in the grid.

In order to obtain expressions for points on the boundaries of the grid, it is necessary to consider the boundary conditions imposed by the problem. First of all, it is assumed that row 5 and column 5 (Figure 8) are far enough from the applied load so that the U and V displacements at these points are zero.

In row 1, the following situation exists. The footing is allowed to undergo an arbitrary settlement, say  $V_0$ . Then  $V_{l-1} = V_{2-1} = V_0$ . The soil directly beneath the footing is assumed to adhere to the base of the footing so that no lateral displacement is possible, or  $U_{l-1} = U_{2-1} = 0.$ 

At points 3-1 and 4-1,  $\sigma_y = \lambda e + 2G \in_y = 0$ . So

$$\lambda \left(\frac{\partial U}{\partial x} + \frac{\partial V}{\partial y}\right) + 2G\left(\frac{\partial V}{\partial y}\right) = \lambda \frac{\partial U}{\partial x} + \alpha \frac{\partial V}{\partial y} = 0$$
 [16c]

Or, in finite difference form, at the point 3-1,

$$\gamma_{31} \left( \frac{U_{41} - U_{21}}{2h} \right) + \alpha_{31} \left( \frac{V_{32} - V_{31}}{h} \right) = 0$$

If  $\mu = 0.25$ , then  $heatharpoonup = \frac{\alpha}{3}$ , and

$$U_{41} - U_{21} + 6(V_{32} - V_{31}) = 0$$
 [17c]

Similarly, for point 4-1,

$$U_{51} - U_{31} + 6(V_{42} - V_{41}) = 0$$
 [17d]

At the centerline of the footing, U = 0 due to symmetry. It may also be seen from symmetry that U (right of centerline) = -U (left of centerline) and V (right of centerline) = V (left of centerline).

If equations [17] are applied to all points in the grid, a system of fifty simultaneous equations in U and V results, twenty-three of which vanish by virtue of the fact that they are identically equal to zero. The remaining twenty-seven simultaneous equations are shown in tabular form in Table 1. These equations can be solved by the digital computer through routine tape L2.

## Determination of Stresses at Grid Points

Once the displacements at the grid points have been determined, the expressions for Hooke's Law can be used to evaluate the stresses at the grid points. Equations [13] can be written

$$\sigma_{\mathbf{x}} = \left[\frac{\mu \mathbf{E}}{(1+\mu)(1-2\mu)}\right] \left[\frac{\partial \mathbf{U}}{\partial \mathbf{x}} + \frac{\partial \mathbf{V}}{\partial \mathbf{y}}\right] + \left[\frac{\mathbf{E}}{(1+\mu)}\right] \frac{\partial \mathbf{U}}{\partial \mathbf{x}}$$

or 
$$\sigma_{\mathbf{x}} = \left[\frac{\mu + (1-2\mu)}{(1+\mu)(1-2\mu)} \left(\frac{\partial \mathbf{U}}{\partial \mathbf{x}}\right) + \frac{\mu}{(1+\mu)(1-2\mu)} \left(\frac{\partial \mathbf{V}}{\partial \mathbf{y}}\right)\right] \mathbf{E}$$
 [18a]

$$\sigma_{y} = \frac{\mu E}{(1+\mu)(1-2\mu)} \left[ \frac{\partial U}{\partial x} + \frac{\partial V}{\partial y} \right] + \frac{E}{(1+\mu)} \left( \frac{\partial V}{\partial y} \right)$$

or 
$$\sigma_{y} = \left[\frac{\mu + (1 - 2\mu)}{(1 + \mu)(1 - 2\mu)} \left(\frac{\partial V}{\partial y}\right) + \frac{\mu}{(1 + \mu)(1 - 2\mu)} \left(\frac{\partial U}{\partial x}\right)\right] E$$
 [18b]

$$\mathcal{T}_{\mathbf{x}\mathbf{y}} = \frac{\mathbf{E}}{2(1+\mu)} \left[ \frac{\partial \mathbf{U}}{\partial \mathbf{y}} + \frac{\partial \mathbf{V}}{\partial \mathbf{x}} \right]$$

or 
$$\mathcal{T}_{xy} = \left\{ \left[ \frac{1}{2(1+\mu)} \right] \left( \frac{\partial U}{\partial y} \right) + \left[ \frac{1}{2(1+\mu)} \right] \left( \frac{\partial V}{\partial x} \right) \right\} E$$
 [18c]

In finite difference form

$$\sigma_{\mathbf{x}} = [k_2(U_{\mathbf{w}} - U_{\mathbf{e}}) + k_1(V_{\mathbf{s}} - V_{\mathbf{n}})] E_{\mathbf{o}}$$
 [19a]

$$\sigma_{v} = [k_{2}(v_{s}-v_{n}) + k_{1}(v_{w}-v_{e})] E_{o}$$
 [19b]

$$T_{xy} = [k_1(U_s - U_n) + (V_w - V_e)] E_0$$
 [19c]

where  $k_1 = \frac{\mu}{2h(1+\mu)(1-2\mu)}$ 

$$k_2 = \frac{\mu + (1-2\mu)}{2h(1+\mu)(1-2\mu)}$$

In its natural state the sand has vertical and horizontal stresses

and acting on it which must be added to the values obtained your from equations [19] to obtain the total horizontal and vertical stress at a point.

The principal stresses  $\sigma_1$  and  $\sigma_3$  can then be obtained from the formulas

$$\sigma_1 = \frac{\sigma_x + \sigma_y}{2} + \sqrt{(\frac{\sigma_x - \sigma_y}{2})^2 + (\tau_{xy})^2}$$
 [20a]

$$\sigma_3 = \frac{\sigma_x + \sigma_y}{2} - \sqrt{\left(\frac{\sigma_x - \sigma_y}{2}\right)^2 + \left(\mathcal{I}_{xy}\right)^2}$$
 [20b]

A program was prepared to perform the operations indicated in equations [19] and [20] on the digital computer. A copy of this program is included in the appendix.

### IV. SETTLEMENT ANALYSIS

## Description of Soil Studied

The material used in the laboratory investigations was Ottawa sand which passed a no. 16 sieve and was retained on a no. 30 sieve.

The sand was tested in a loose and a dense state. To achieve the loose state, the sand was simply poured into the mold with no compaction. The dense state was obtained by compacting the material in five layers as it was placed in the mold.

## Elastic Method

Triaxial tests. A series of triaxial tests was performed to determine the constants  $C_I$  and  $C_{III}$  for loose and dense sands. All specimens were consolidated under a principal stress ratio of 2.0 ( $k_O = 0.5$ ) before application of hydrostatic or deviator stress. A summary of the tests performed is given in Table 2. The stress-strain curves obtained from these tests are shown in Figures 11 and 12. From the stress-strain curves, the values of  $C_I$  and  $C_{III}$  were determined as described in section II. Curves demonstrating the relationship between the elastic constants and the minor principal stress (for compacted sand only) are shown in Figures 13.

Settlement calculations. The settlement analysis was carried out in the following manner. First of all, it was noted that the order of magnitude of the constant  $C_{\overline{III}}$  is very small compared to  $C_{\overline{I}}$ .

The settlement contributed by the term  $C_{III}$  ·  $\Delta \sigma_3$  is therefore negligible and was omitted in the calculations.

The actual mechanism of settlement is not perfectly reproduced in the laboratory tests; that is, in the laboratory tests, the stresses  $\Delta \sigma_3$  and  $(\Delta \sigma_1 - \Delta \sigma_3)$  are applied in two separate stages, whereas in a loaded soil mass they occur simultaneously. It is therefore necessary to determine the value of  $C_I$  that most nearly represents the true condition.

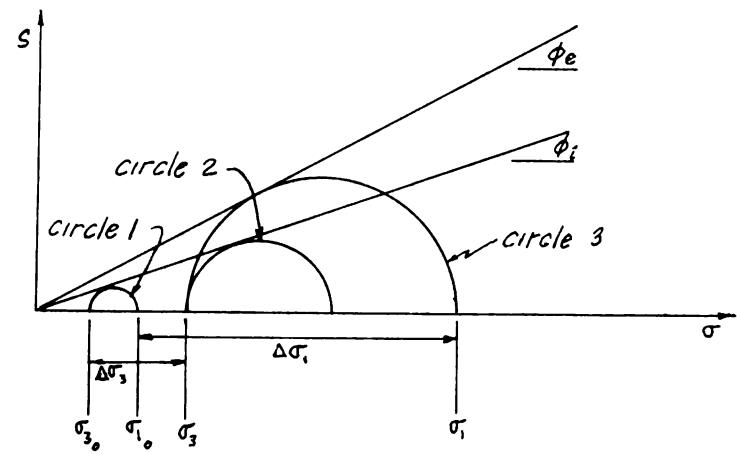


Figure 10: Mohr's circle representation of stresses in sand.

In Figure 10, circle 1 represents the initial state of stress in the sand mass. As the footing load is applied,  $\sigma_3$  and  $\sigma_1$  increase by  $\Delta \sigma_3$  and  $\Delta \sigma_1$  so that the final state of stress is represented by circle 3. Circle 2 represents the state of stress in a triaxial specimen consolidated to the final  $\sigma_3$  while the principal stress ratio remains unchanged ( $\sigma_3 = 0.5 \sigma_1$ ). Then the deviator stress is increased and the Mohr's circle increases in size until it coincides with circle 3. The increase in strain under the increasing deviator stress was used to calculate  $\sigma_1$ .

 $C_{\rm I}$  is chosen as that which corresponds to the value of  ${}_3$  which exists at the point under consideration in the sand mass after application of the footing load. Although this choice of  $C_{\rm I}$  most nearly represents the stress changes taking place in the sand mass, it is not strictly correct. It omits the additional settlement which takes place before  $C_{\rm I}$  builds up to its final value. However, the error due to this omission is small.

The settlement of a continuous footing 15 feet wide, supporting a load of l kg/cm<sup>2</sup> was calculated by the method outlined in section II, using the results of the triaxial tests. The values of  $\Delta \sigma$  and  $\Delta \sigma$  as determined by means of Boussinesq's equations are given in Table 3. As calculated by the elastic method, the settlement is 21.8 cm at the centerline of the footing. (See Table 4.)

# Consolidation Method

A standard consolidation test was performed on a sample of Ottawa sand in the loose state. The load-settlement curve obtained is shown in Figure 14.

The settlement under a continuous footing 15 feet wide, supporting a load of 1 kg/cm<sup>2</sup> was calculated using equations [12]. The calculated settlement is 0.578 cm.

### Numerical Method

In order to make use of the equations derived in section III,

it is necessary to establish the values of E,  $\gamma$  and  $\alpha$  at each of the grid points. A rather complete set of triaxial test data has been published by Chen (3) from which one can plot the variation of the modulus of elasticity in a sample of sand with the minor principal stress. Figure 17 shows the E versus  $\sigma_3$  curves one obtains from Chen's data.

According to the curves in Figure 15, the relationship between E and  $\sigma_3$  is practically a straight line for low stresses. This can be expressed as E = k  $\sigma_3$  where k is some constant. Actually  $\frac{E}{\sigma_3}$  is not exactly constant, but varies somewhat with the deviator stress. However, the variation is small and may be ignored for simplicity. The lower portion of the curves was used to determine the value of k because this portion represents the range of stresses encountered in the problem.

The value of k was determined from the curves for a medium sand. The average value of k for these curves is 2500.

With the value of k established, it remains to obtain an estimate of  $\sigma_3$  so that starting values of E,  $\lambda$  and  $\alpha$  can be determined for each of the grid points. A reasonable estimate of  $\sigma_3$  can be obtained by the use of Boussinesq's equations.  $\sigma_3$  was evaluated in this manner for a load of l kg/cm<sup>2</sup> acting on the footing. The stresses obtained and the resultant constants E,  $\lambda$  and  $\alpha$  for all grid points are given in Table 3.

The values of the constants E, 7 and a from Table 3 were substituted into the equations given in Table 1. These equations were solved by the digital computer, giving the values of the displacements U and V at all points in the grid. Using these values of U and V, the stresses at the grid points were determined by means of equations [19] and [20]. This operation was also performed on the digital computer.

After the values of  $\sigma_3$  have been computed, new values for E can be obtained from the relationship  $E = k \sigma_3$  and the entire procedure repeated until the values of  $\sigma_3$  converge. In this manner, all values of stresses and displacements in the grid system can be evaluated for the given settlement. However, in this investigation it was not possible to carry out the successive approximation because of the lack of storage space. Only the first approximation was obtained.

The investigation was made for a rigid, continuous strip footing 15 feet wide, with a given settlement of 1 cm. It was assumed that  $\mu$  = 0.25 and E = 2500  $\sigma_3$ .

The distribution of stresses and displacements obtained from this investigation is shown in Figures 16 and 17.

### V. CONCLUSIONS

The settlements calculated by the different theories are listed in Table 4. It is obvious that the different methods of settlement analysis give very different results.

The settlement calculated by the consolidation method is far too small. Although the sand is very loose the settlement is only 0.578 cm. The answer is unreasonable. As was pointed out, the conditions of stress and strain in the consolidation test are not consistent with actual conditions. Therefore, the consolidation method of analysis should not be applied to sands.

The settlement obtained by the elastic analysis is larger than those commonly observed (10). If one examines the validity of this method, it is noted that certain inconsistencies exist. Because triaxial tests, in which  $\sigma_2$  equals  $\sigma_3$ , are used in the calculation of settlement, the assumption that the footing is circular in shape is inherent in the development. The principal stresses  $\sigma_2$  and  $\sigma_3$  are not equal under a continuous footing. Rather  $\sigma_2$  is greater than  $\sigma_3$ , which means that the application of this method to a continuous footing results in an overestimation of settlement. This fact was borne out in recent tests conducted under the direction of Bishop at Imperial College (14). Bishop has developed an apparatus which is capable of measuring the stress-strain characteristics of sand under the condition of plane strain. It has been found that the vertical strain in a sample of sand is reduced considerably when loaded under plane strain conditions.

Another factor is that the footing is assumed to be perfectly flexible. For rigid footings, the settlement is much smaller than that at the center of flexible ones.

Field observations of the settlement of circular foundations
resting on loose sand at Drammen, Norway (7) indicate that the
magnitude of settlement obtained in this investigation is quite reasonable.

It may be concluded therefore, that the elastic analysis is capable of producing good results provided that the stress-strain conditions of the tests from which the elastic constants are obtained are the same as those under the actual footing.

The results obtained by the numerical method developed in this thesis are quite promising. The contact pressure distribution obtained agrees in general with that observed in model tests. [See for instance, Bond (1)].

To evaluate the calculated settlement, it is necessary to examine the value of k adopted in the calculations. The constant k is determined under the condition that  $\sigma_2$  equals  $\sigma_3$ . The error involved is the same as that for the elastic analysis. To be strictly correct, k should be determined from the stress-strain characteristics of sand under plane strain conditions. This necessitates the use of a testing apparatus similar to that developed by Bishop which is, as yet, not in general use.

The reliability of k equal to 2500 can be examined from another point. Chen's data, from which this k was obtained can be compared with the elastic constants from the triaxial tests carried out in this investigation. It is possible to compute, from the results of the triaxial tests, the values of E and  $\mu$  of the sand for various  $\sigma_3$ . This was done and

the results presented in Figures 18 and 19. If one compares the values of E obtained from these tests with those obtained by Chen, one finds a rather large discrepancy. There are two reasons for this.

With Chen's data a k of 2500 was obtained by taking the secant modulus at 0.50D. Whereas, in the present series of tests these constants represent the tangent moduli at stresses considerably above the principal stress ratio of 2.0. For a  $\phi$  of 30°, this principal stress ratio corresponds to approximately 0.50D. In order to compare the moduli at approximately equal shear stresses, k should be taken from the curve corresponding to 0.75D in Chen's data. Then one finds that k = 800 which is in much better agreement with that obtained in the triaxial tests performed in this investigation. For a k of 800 the settlement is approximately 3 cm for the same contact pressure. The range in settlement then, is between 1 cm and 3 cm which is in reasonable agreement with observed results.

# TABLE 1

SIMULTANEOUS EQUATIONS IN U AND V

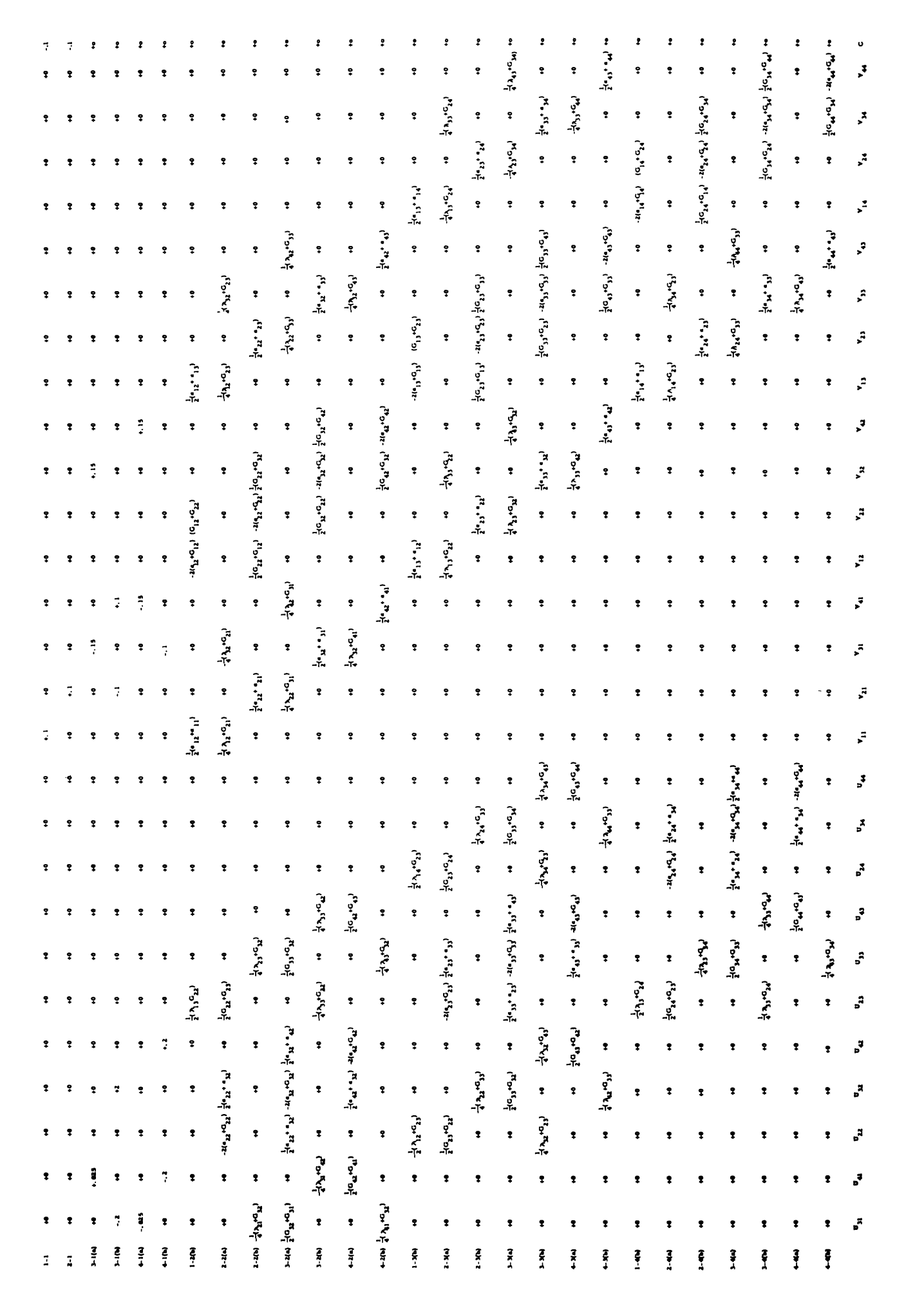
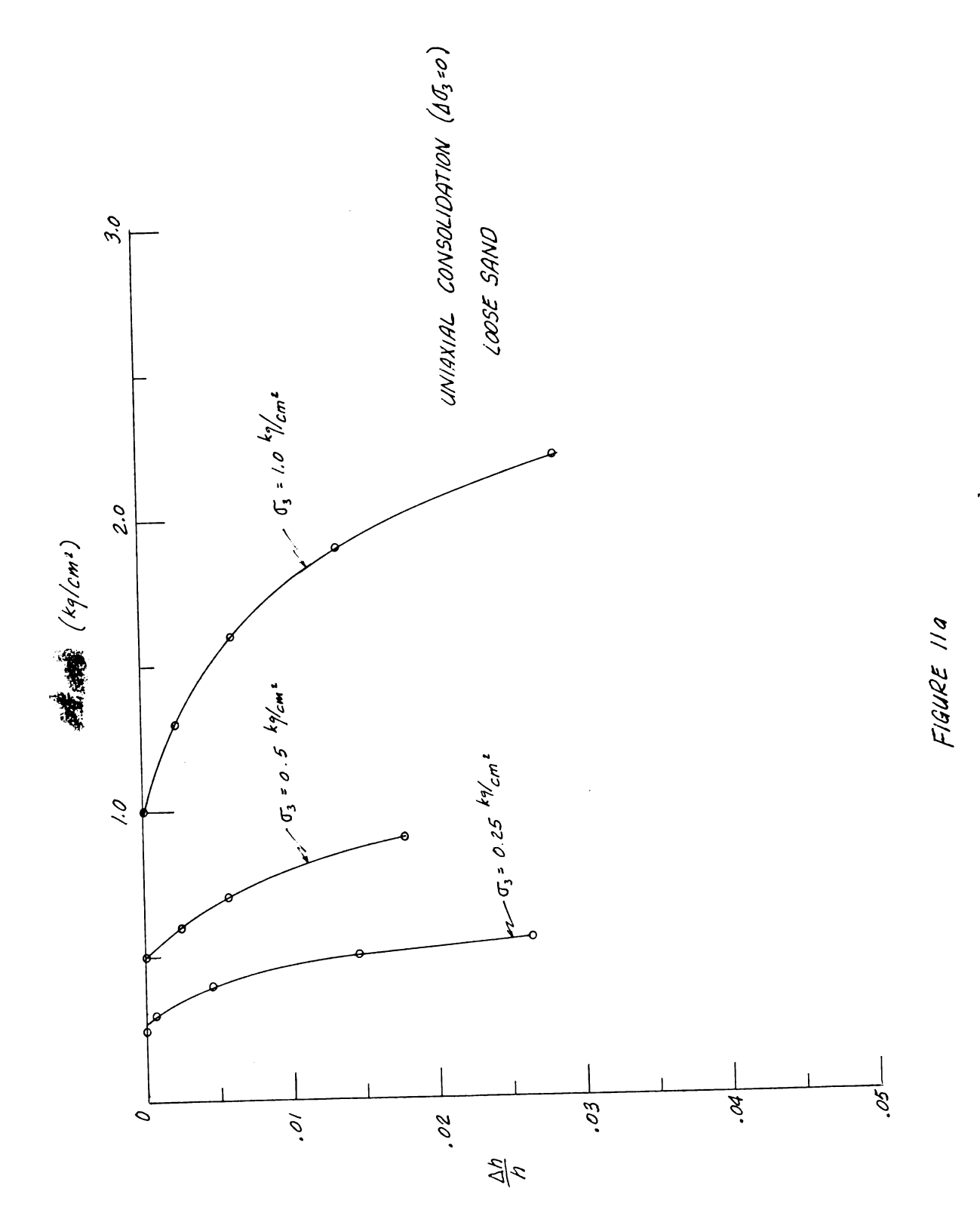
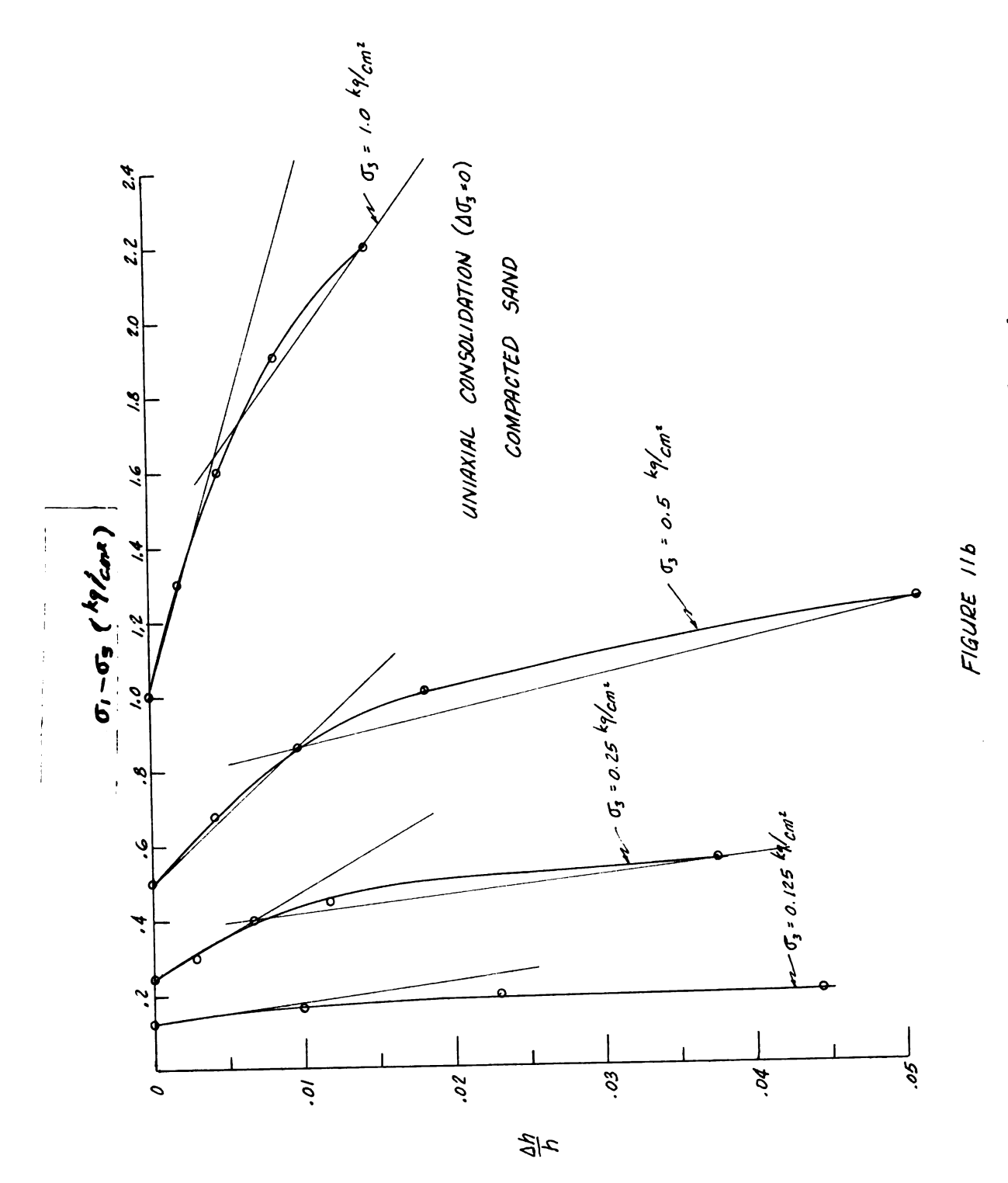


TABLE 2 TRIAXIAL TESTS

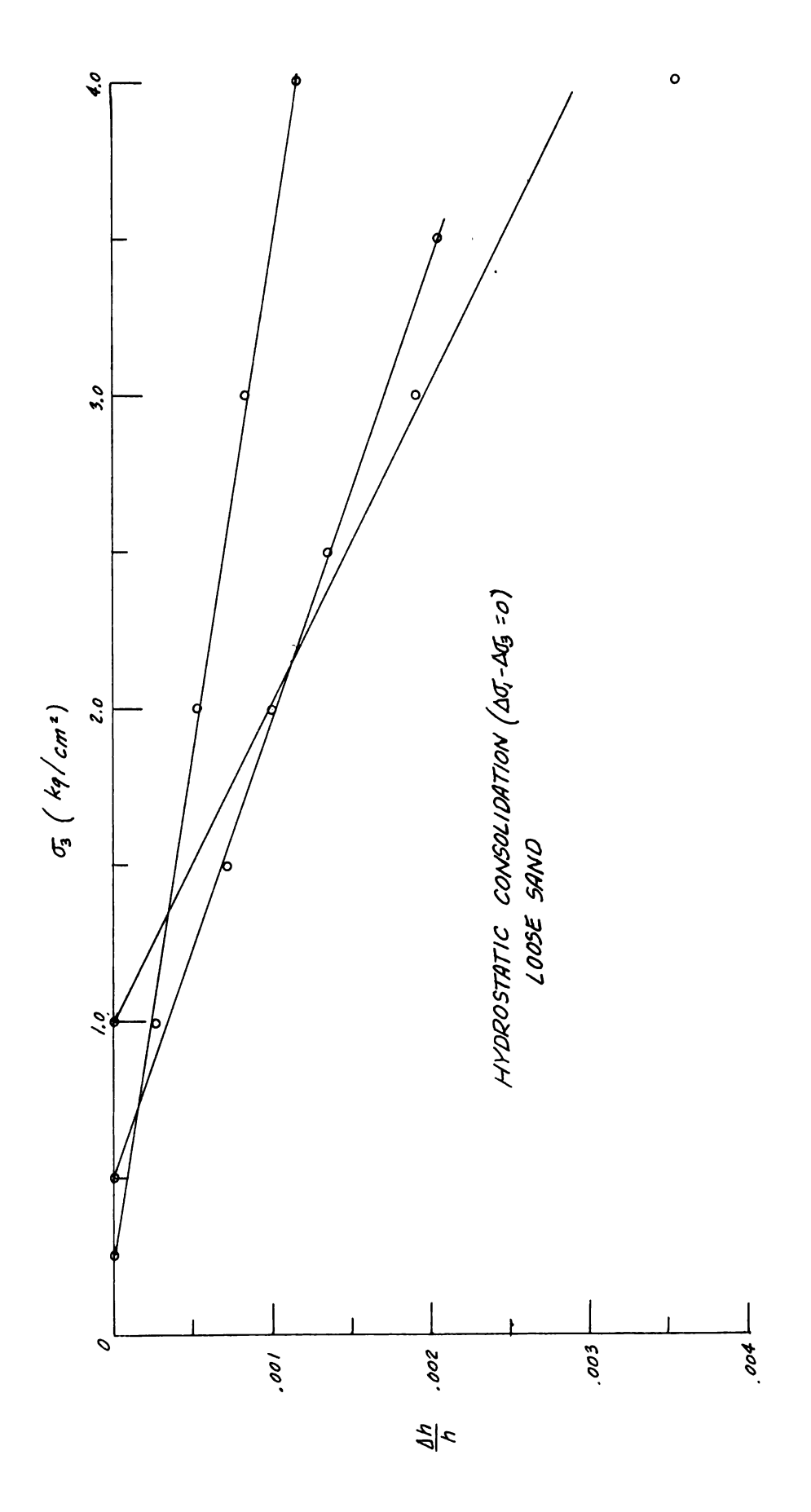
1	Sample	Sample dimensions	1 1 1 1	Hy	drostatic c	Hydrostatic consolidation	u	Uniaxial consolidation-	ial consolie	lation
Sample	Initial	average cross-	Void	$\sigma_3 (kg/cm^2)$	cm <sup>2</sup> )	$\sigma_1^{(kg/cm^2)}$	cm <sup>2</sup> )	$\sigma_3 = \text{const.}$	$q_1(kg/cm^2)$	n <sup>2</sup> )
o N	height (cm)	sectional area (cm <sup>2</sup> )	ratio	from	ţ	from	to	(kg/ cm²)	from	to
1	9.08	11.38	0.527					0.125	0.250	0.323
2.	60.6	11.85						0.250	0.500	0.800
3	8.89	10.90	0.528					0.500	1.000	1.736
4	9.17	10.52						1.000	2.000	3, 200
Ŋ	60.6	10.98		0.25	4.00	0.50	4.25			
9	8.97	10.70		0.50	4.00	1.00	4.50			
7.	60.6	11.10		1.00	4.00	2.00	5.00			
8.	8.26	9.63	0.603					0.250	0.500	0.800
6	7.82	10.00						0.500	1.000	1.400
10	8.12	11,15						1.000	2.000	3, 200
11	8.73	10.62	0.615	0.25	4.00	0.50	4.25			
12	8.06	9.97	0.561	0.50	3.50	1.00	4.00			
13	8.06	10.00	0.627	1.00	4.00	2.00	5.00			



Stress-strain curves for loose sand

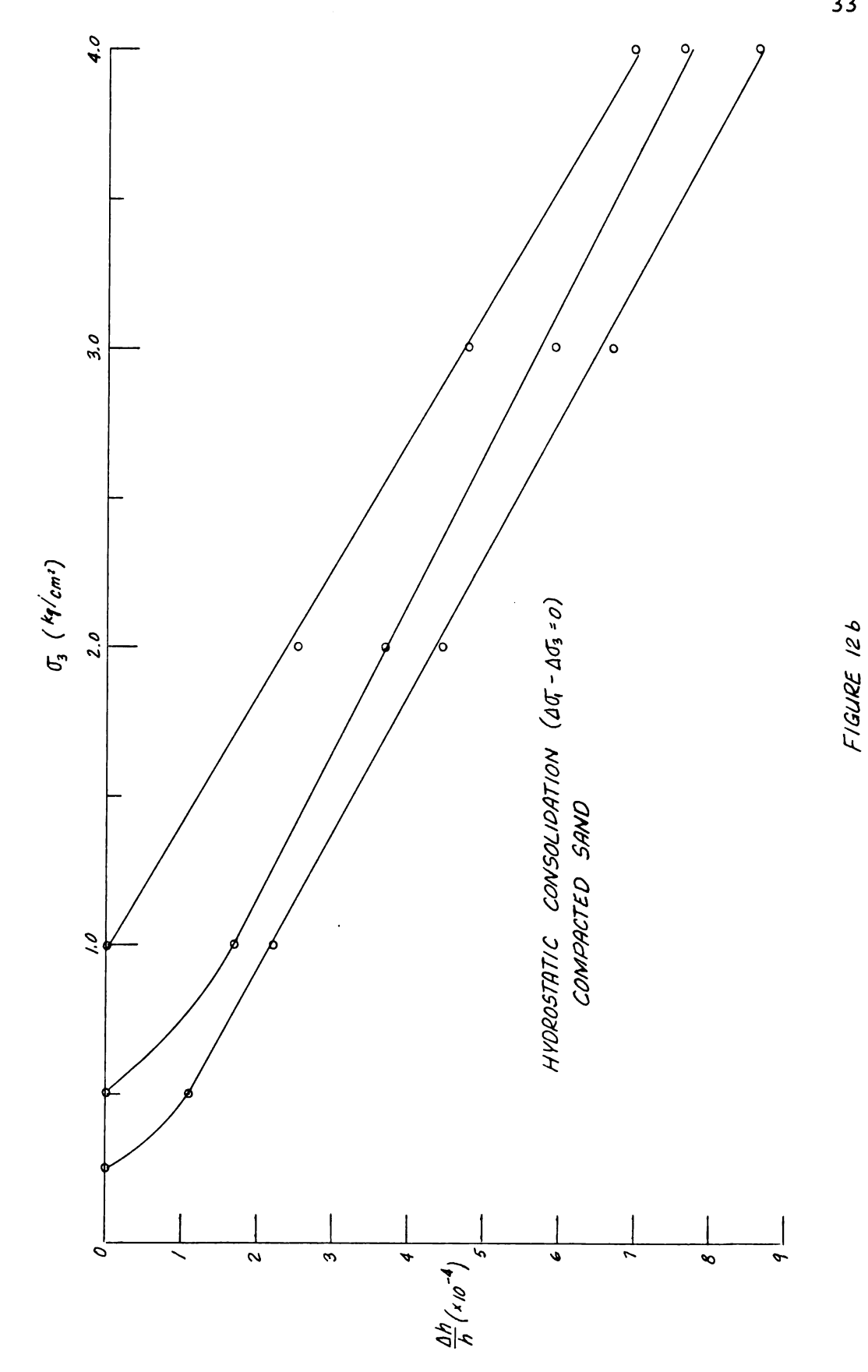


Stress-strain curves for compacted sand

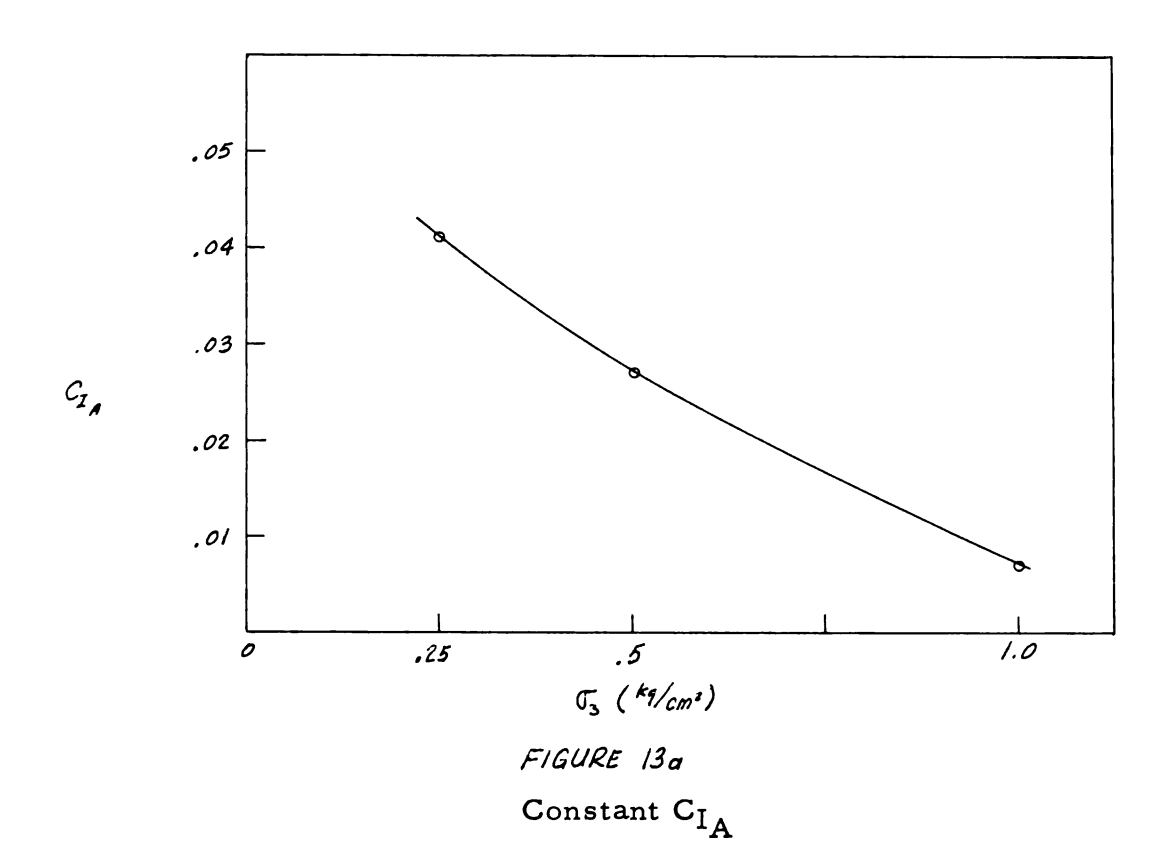


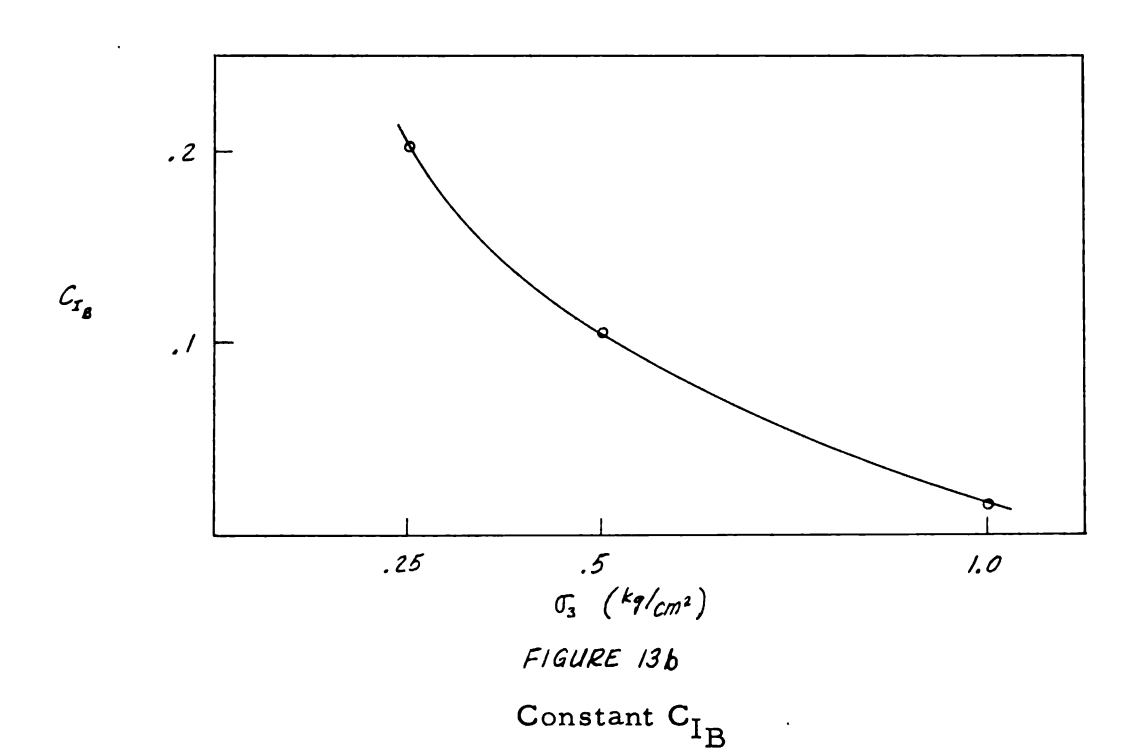
Stress-strain curves for loose sand

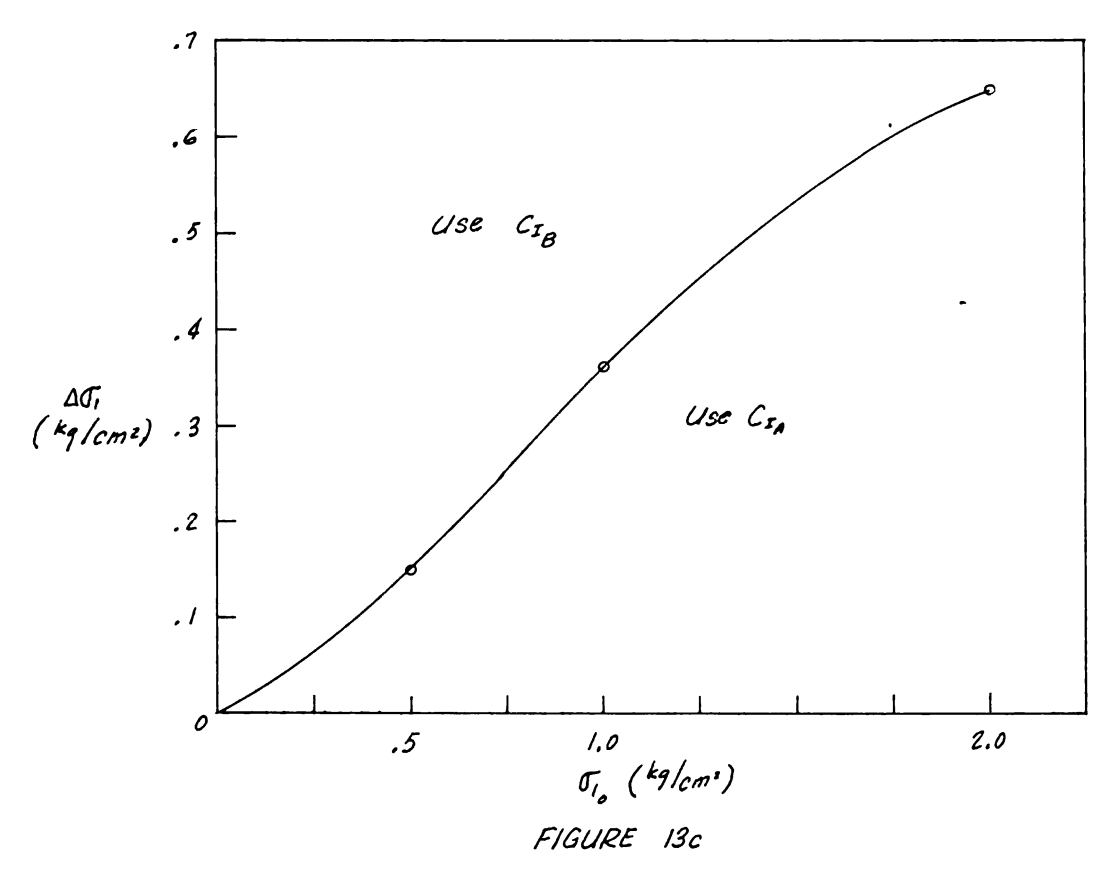
FIGURE 120

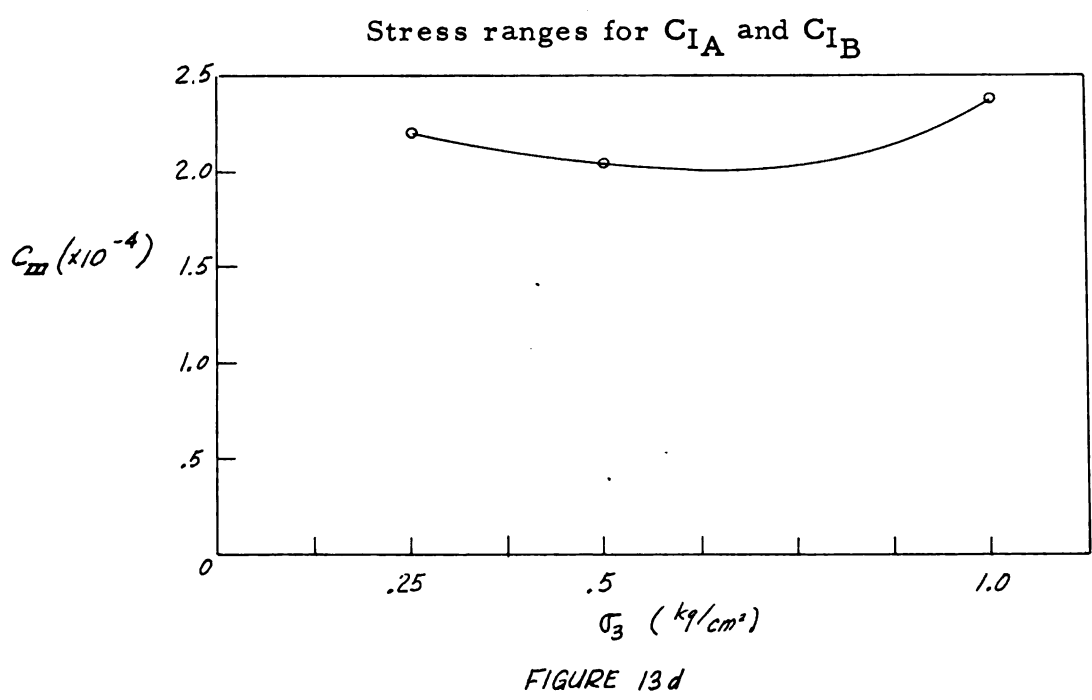


Stress-strain curves for compacted sand









Constant C

TABLE 3. STRESSES, E, A AND & AT GRID POINTS FROM BOUSSINESQ'S EQUATIONS

Pt.	Q Px	P <sub>×</sub> °	۵ ۲>	P <sub>X</sub>	$\mathcal{L}_{xy}$	<b>ь</b> ×.	P <sub>2</sub>	P_L	P.	E G * 2500	λ=G . 4E	a=3G
1-1	*. 600	0	*1.000	0	0	009.	1.000	1.000	009.	1500	009	1800
2-1	*. 600	0	*1.000	0	0	009.	1.000	1.000	009.	1500	009	1800
3-1	0	0	0	0	0	0	0	0	0	0	0	0
4-1	0	0	0	0	0	0	0	0	0	0	0	0
1-2	. 522	. 131	006.	. 262	0	. 653	1.162	1.162	. 653	1630	652	1960
2-2	. 264	. 131	. 664	9	192	. 395	926.	. 763	. 557	1440	277	1730
3-2	.256	. 131	. 221	. 260	220	. 387	. 483	099.	. 210	526	210	631
4-2	. 167	. 131	. 037	9	083	. 298	. 299	. 325	.272	089	272	817
1-3	. 106	. 262	. 700		0	. 368	1.224	1.224	. 368	920	368	1105
2-3	. 136	. 262	619.		163	. 398	1.143	. 971	. 570	1425	240	1712
3-3	. 177	. 262	. 320	. 524	180	. 439	. 844	.910	. 381	953	381	1142
4-3	. 182	. 262	. 130	. 524	130	. 444	. 654	. 716	. 382	955	382	1145
1-4	.050	. 392	. 520	. 784	0	. 442	1.304	1.304	. 442	1105	442	1328
2-4	. 080	392	. 464	. 784	072	. 472	1.248	1.002	. 718	1798	718	2160
3-4	.110	. 392	. 316	. 784	138	. 502	1.100	1.309	. 635	1589	635	1907
4-4	. 139	. 392	. 175	. 784	155	. 531	636.	. 959	. 431	1078	432	1294
1-5	. 040	. 523	. 424	1.046				1.470	. 563			
1-6	.030	. 654		1,308				1.648	. 684			
1-7	.020	. 785	300	1.570				1.870	. 805			

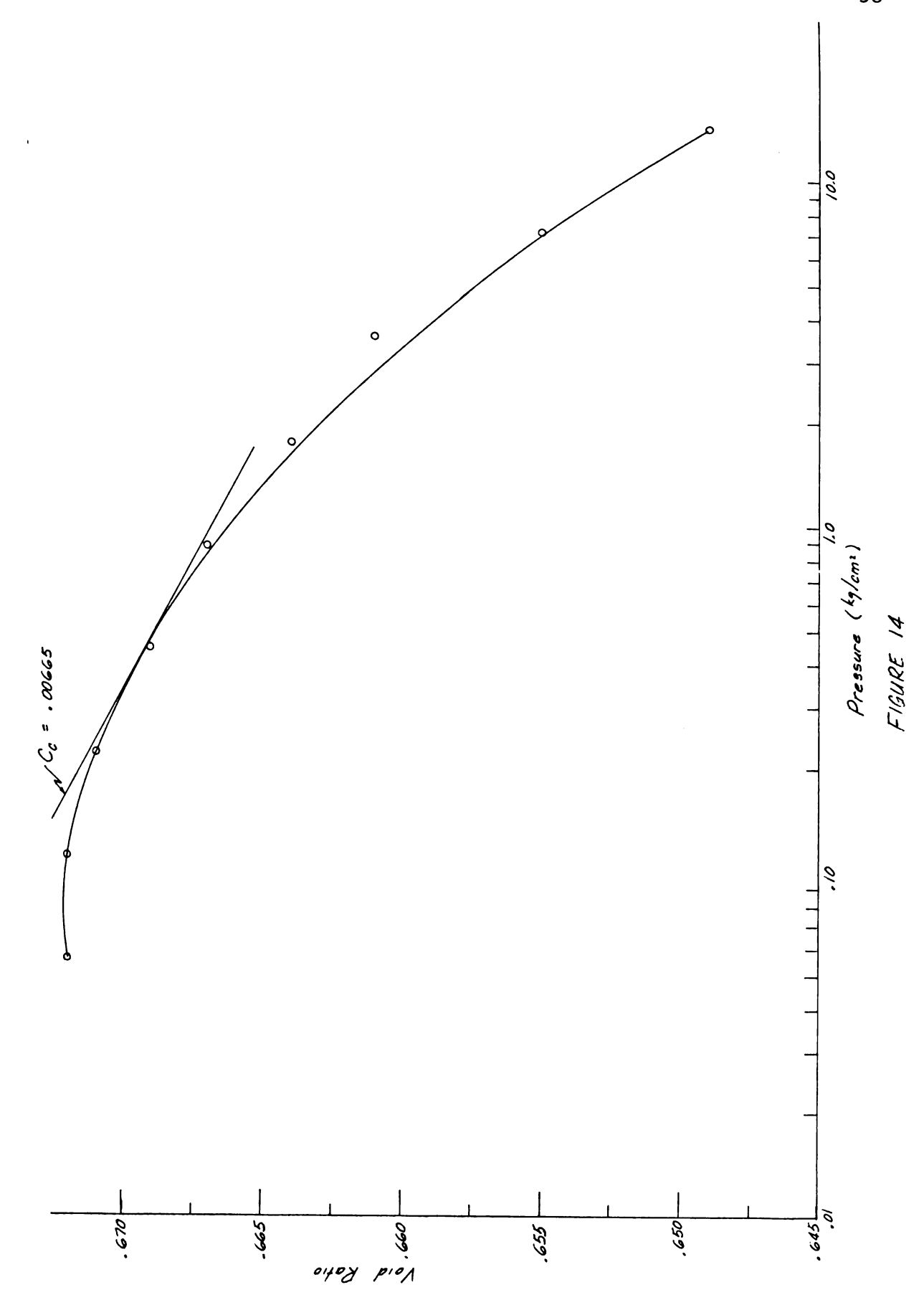
\*Estimated.

 $<sup>\</sup>gamma = 105 \text{ pcf}$ 

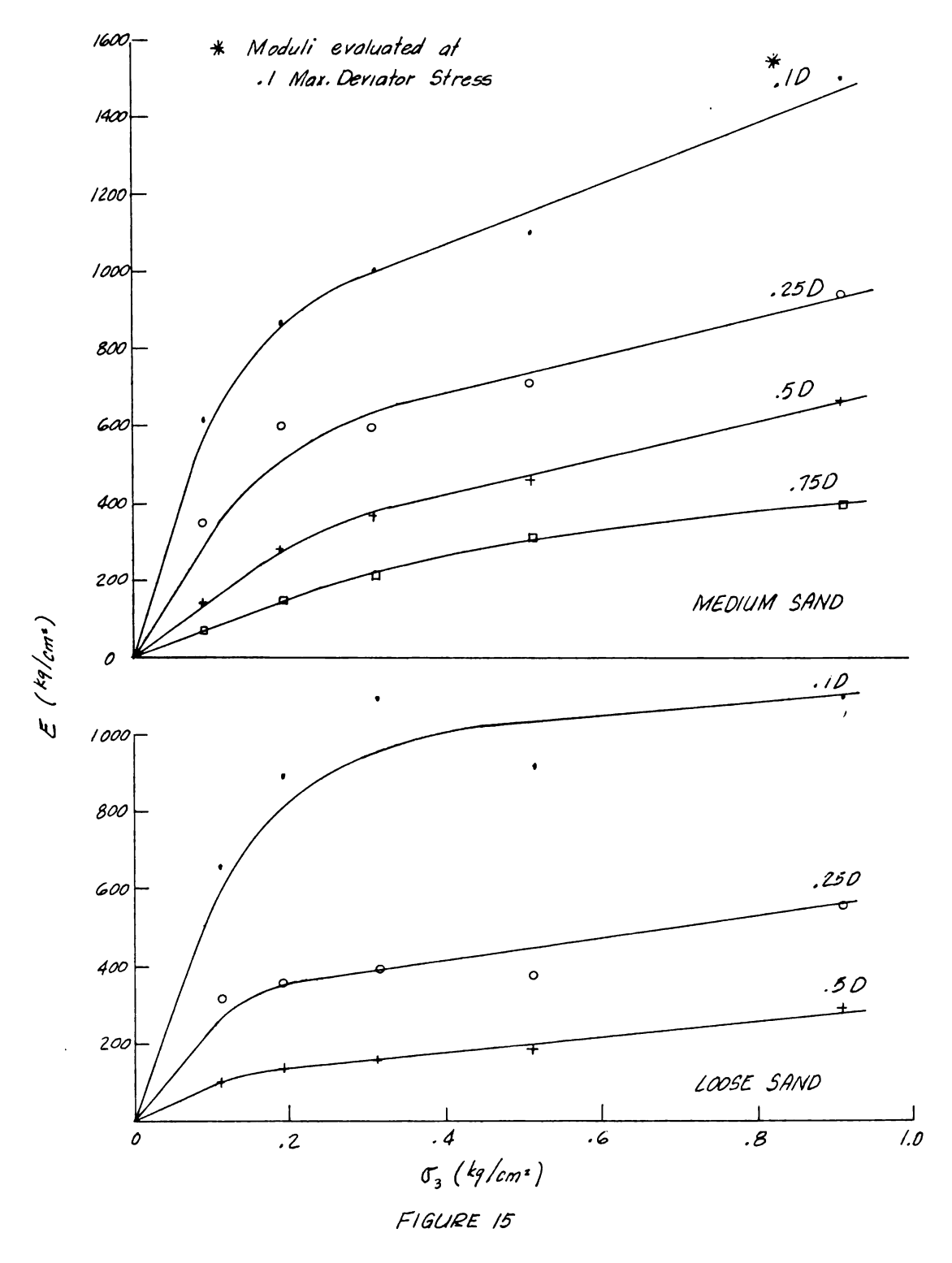
TABLE 4

RESULTS OF SETTLEMENT COMPUTATIONS

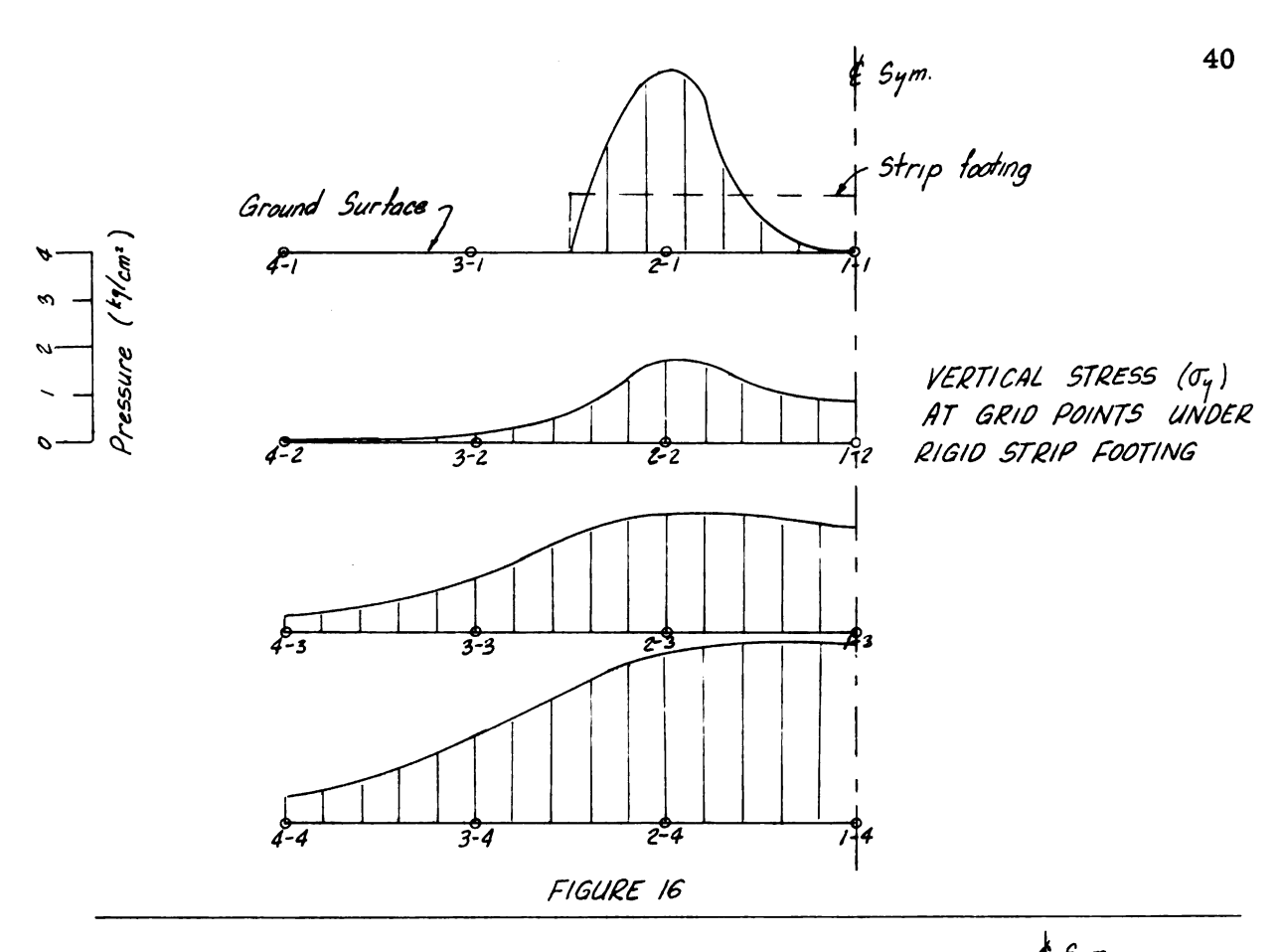
Description of footing	Soil type	Method of settlement analysis	Contact pressure	Settlement
Strip footing, 15' wide, flexible	Ottawa sand Passing #16 sieve Retained on #30 sieve	Elastic analysis	1 kg/cm <sup>2</sup>	21.8 cm
Strip footing, 15' wide, flexible	Ottawa sand Passing #16 sieve Retained on #30 sieve	One-dimensional consolidation method	$1  \mathrm{kg/cm}^2$	0. 578 cm
Strip footing, 15 ft. wide, rigid	Medium sand	Numerical method	Shown graphically in Figure 16	l cm



Pressure-void ratio curve for loose sand



The secant modulus



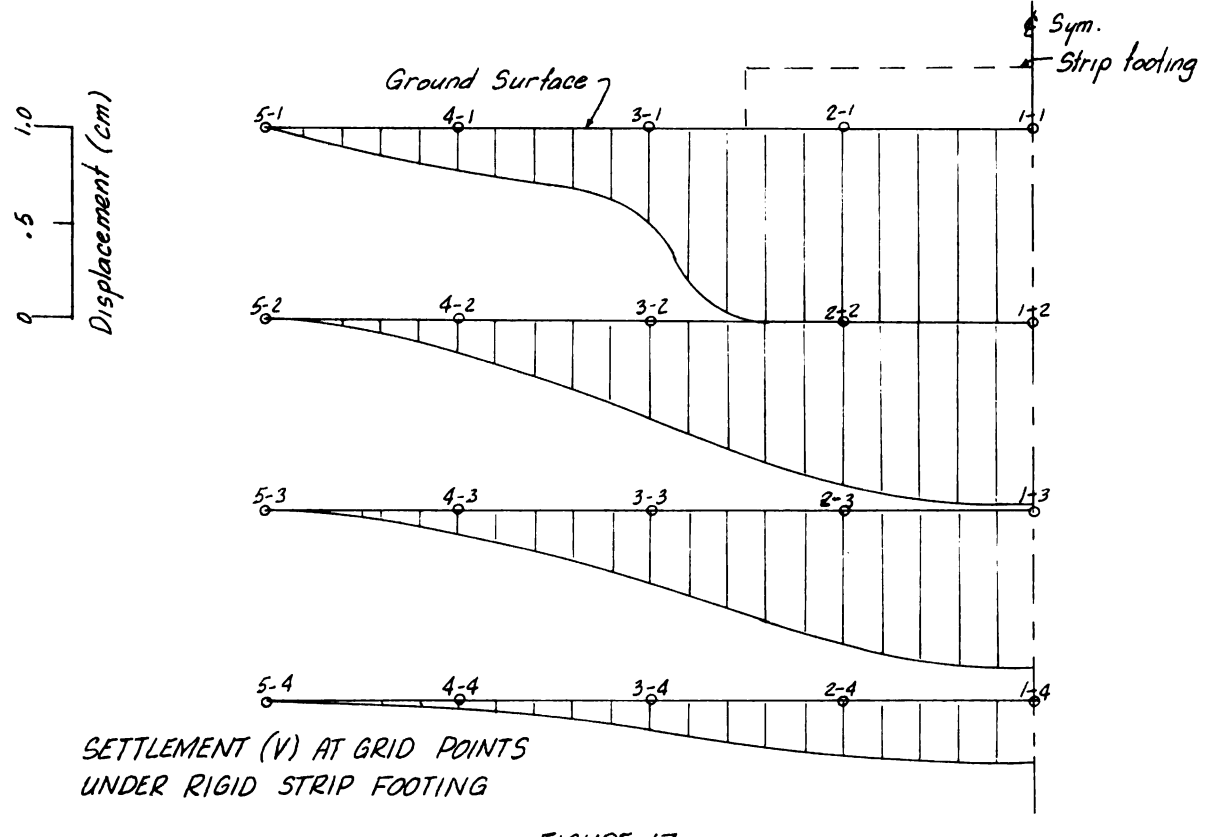
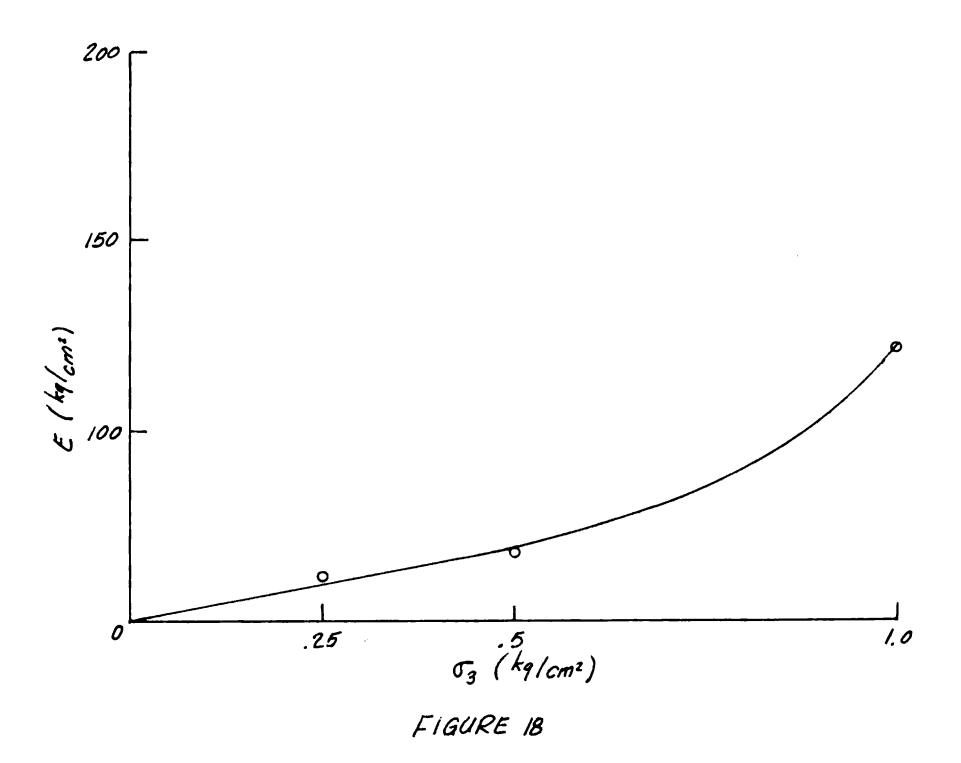
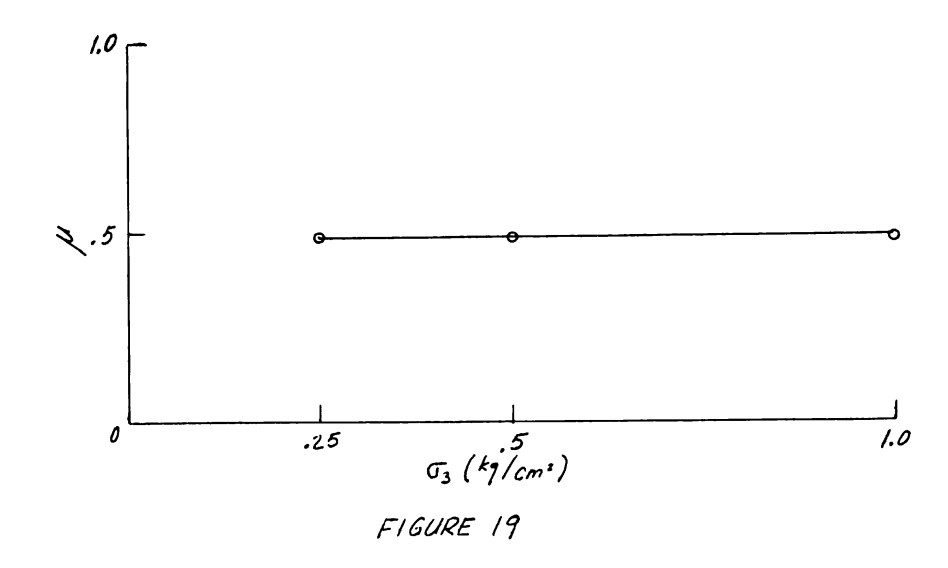


FIGURE 17



The tangent modulus



Poisson's ratio

## APPENDIX

## Computer Tape for $\sigma_{\mathbf{x}}$ , $\sigma_{\mathbf{y}}$ , $\tau_{\mathbf{x}\mathbf{y}}$ and $\sigma_{\mathbf{x}}$

8002840001	0020+
8002840002	001F 001F
1902626000	003F 003F
8002840000	002F 002F
L400140001	003F 003F
80028403 <b>F</b> 6	003F 003F
-5000263L6	001F 000F
81004263FJ	001F 001F
4000122000	0063F 0063F
7J3LFL4001	L5308F L0306F
40001263L8	L5413F L0401F
L4002263F-	0014F 0015F
423FFL5001	000F 001F
L4000L4000	00200+
263F-L03LL	-5 <b>F4</b> 68L
703LL-53 <b>F</b> 7	L44L4211L
4000081004	814FL025L
50000L43LL	221 <b>0</b> L <b>402F</b>
323FLL43L <b>0</b>	<b>L</b> 5 <b>F</b> 661 <b>F</b>
423L5L5001	101F-JF
L400026000	40FL1F
40002L03L4	401FL52F
423L8233L9	<b>40F</b> L58L
5000140000	L44L468L
U3F9L43L4	L52 <b>F</b> 427L
423F9L43L8	L023L32 <b>F</b>
423L800027	L524L401F
800080000N	41 F81 4F
40001273L1	L025L402 <b>F</b>
465 <b>F</b> 66 <b>0</b> 4-8	326LL424L
7LLLLLLL6	40F814F
223L-00001	501 <b>F4</b> 02 <b>F</b>
	L025L323L
	7525L-5 <b>F</b>
	401F5025L
	75 <b>F</b> 0039 <b>F</b>
	L42F2616L
	000F002F
	00F005F
	000F0010F
	000-00-0

00230+	50300F 500L	4026L L528L
40FL527L	262 <b>00F</b> 242L	L420F 4028L
-4 <b>F</b> 4225L	50400F 502L	L521F L020F
461L402 <b>F</b>	262 <b>00F</b> 244L	<b>4021F</b> 3626L
92961 <b>F</b> 366L	50490 <b>F</b> 504L	L526L L422 <b>F</b>
L5F366L	262 <b>00F</b> 246L	4026L L528L
92706F226L	50500F 506L	L422F 4028L
92961 <b>F</b> 5026L	26200F 248L	L523F 4021F
228L461L	50700F 508L	L524F L020F
7526LL51L	26200F 24100F	4024F 3626L
L019L327L	00100+	L5600F L0616F
-5F401F	L5308F L0306F	L4700F L0716F
L52F006F	40398F 50398F	40398F 50398F
50L3214L	7J490F 40398F	75398F 102F
L7F661F	L5413F L0401F	40399F 41498F
2315L671 <b>F</b>	40399F 50399F	50632 <b>F</b> 75632 <b>F</b>
L7F-4F	7J491F L4398F	L4399F 5050L
40F50F	40600F L56L	2626 <b>0F</b> 2652L
7526L0036 <b>F</b>	L425F 406L	40399F L5600F
824F1040F	L50L L420F	L4616F L4700F
-410F40F	400L L53L	L4716F 101F
-410F 40F	L420F 403L	L4399F 40399F
L51LL016L	L521F L020F	50399 <b>F</b> 75500 <b>F</b>
461L009F	4021F 360L	40648F 2658L
3623L92961F	L50L L422F	L557L L425F
L52FL019L	400L L53L	4057L L544L
462F0010F	L422F 403L	L420F 4044L
3216L22F	L523F 403L L523F 4021F	L549L L420F
00F0010F	L524F L020F	4049L L552L
821013F001F	4024F 160L	L431F 4052L
821013F001F	L523F 4024F	L431F 4032E L553L L420F
003/01		
00260+	L5493F 40490F	4053L L545L
401F+5F	L5492F 40491F	L420F 4045L
428L511 <b>F</b>	L528F 400L	L554L L425F
101F-JF	L529F 403L	4054L L556L
402F50F	L526F L020F	
L51 <b>F</b> 662 <b>F</b>	4026 <b>F</b> 360L	L431 <b>F</b> 4056 <b>L</b>
-5FL02F	L5313F L0301F	L530F L020F
101F368L	40398F 2628L	4030F 3644L
L42F263L	L5408F L0406F	92131 <b>F</b> L56 <b>00F</b>
L52 <b>F</b> 22 <b>F</b>	L4398F 40398F	5299 <b>F</b> 5073L
	50398F 7J493F	2623 <b>0F</b> L572L
0050+	40632F L531L	L431F 4072L
	L425F 4031L	L527F L020F
	L526L L42 <b>0F</b>	4027F 3672L
		92131F <b>0FF</b>
		2450N

## BIBLIOGRAPHY

- 1. Bond, Douglas, "The Use of Model Tests for the Prediction of Settlement under Foundations in Dry Sand." Ph. D. thesis, University of London, 1956.
- 2. Boussinesq, J., "Applications de Potentiels a l'Etude de l'Equilibre et des mouvement des Solides Elastiques." Gauthier-Villars, 1885.
- 3. Chen, Liang-Sheng, "An Investigation of Stress-Strain and
  Strength Characteristics of Cohesionless Soils by Triaxial
  Compression Tests." Proceedings of the Second International Conference on Soil Mechanics and Foundation
  Engineering, Vol. 4, 1940.
- 4. Hough, B. K., "Compressibility as the Basis for Soil Bearing Value," Proceedings of the American Society of Civil Engineers, August, 1959.
- 5. Jurgenson, Leo, "The Application of Theories of Elasticity and Plasticity to Foundation Problems." Journal of the Boston Society of Civil Engineers, July, 1934.
- 6. Myerhoff, G. G., "The Bearing Capacity of Sand." Ph. D. thesis, University of London, 1950.
- 7. Simons, N., "Settlement of Structures on Sand." Internal Report No. F. 31, Norges Geotekniske Institute, March, 1956.
- 8. Taylor, Donald W., Fundamentals of Soil Mechanics, John Wiley & Sons, Inc., 1948.
- 9. Terzaghi, Karl, Theoretical Soil Mechanics, John Wiley & Sons, Inc., 1943.
- 10. Terzaghi, Karl and Peck, Ralph B., Soil Mechanics in Engineering Practice, John Wiley & Sons, Inc., 1948.
- 11. Timoshenko, S. and Goodier, J. N., Theory of Elasticity, McGraw-Hill Book Company, Inc., 1951.
- 12. Tschebetarioff, Gregory P., Soil Mechanics, Foundations, and Earth Structures, McGraw-Hill Book Company, Inc., 1951.

- 13. Waterways Experiment Station, Investigations of Pressures and

  Deflections for Flexible Pavements, Report No. 4,

  Homogeneous Sand Test Section, Technical Memorandum
  No. 3-323, December, 1954.
- 14. Wood, C. C., "Shear Strength and Volume Change Characteristics of Compacted Soil under Conditions of Plane Strain."
  Ph. D. thesis, Imperial College, 1957.

## ROOM USE ONLY

FORE CHLY

MICHIGAN STATE UNIVERSITY LIBRARIES

3 1293 03046 3685